11-30-2018

Cross-talk Between Different DNA Sensors in the Cytosol

Ishita Banerjee
University of Connecticut - Storrs, ishitabanerjee09@gmail.com

Cross-talk Between Different DNA Sensors in the Cytosol

Ishita Banerjee, PhD.

University of Connecticut, 2018

Abstract

DNA released into the cytoplasm as a consequence of microbial infection or pathology can be recognized by the host sensor, Absent in melanoma (AIM) 2 that leads to the assembly and activation of the inflammasome complex and cyclic GMP-AMP synthase (cGAS) that induces type-I Interferon (IFN) production. Inflammasome activated caspase-1 cleaves gasdermin-D leading to pore-formation in the plasma membrane that subsequently results in pyroptosis. In this study we found that activated gasdermin-D negatively regulates cGAS-induced type-I IFN production in a pyroptosis and interleukin (IL)-1β and IL-18 independent manner. Mechanistic studies showed that gasdermin-D pore formation lead to a loss of intracellular potassium (K^+) concentration that suppressed the production of cGAS-induced type-I IFN. Therefore, we report a novel regulatory mechanism for cGAS/STING-induced type-I IFN that may have profound therapeutic implications in autoimmune diseases and anti-tumor immunotherapy.

Cross-talk Between Different DNA Sensors in the Cytosol

Ishita Banerjee

B.S., University of Delhi
M.S., University of Delhi

Major Advisor: Vijay Rathinam, D.V.M, PhD.

Associate Advisor: Anthony Vella, PhD.

Associate Advisor: Kamal Khanna, PhD.

A Dissertation Submitted in Partial Fulfillment of the Requirements for the

Degree of
Doctor of Philosophy

at the

University of Connecticut
2018

2018

APPROVAL PAGE

Doctor of Philosophy Dissertation

Cross-talk Between Different DNA Sensors in the Cytosol

Presented by
Ishita Banerjee

Major Advisor

_____
Vijay Rathinam, D.V.M., PhD.

Associate Advisor

_____
Anthony Vella, PhD.

Associate Advisor

_____
Kamal Khanna, PhD.

University of Connecticut
2018

Acknowledgements

I would like to express my heartfelt gratitude to Vijay for entrusting me with an interesting research question. I thank him for his through mentorship and guidance throughout my thesis work. I have not only imbibed the principles of conducting scientific research but also learnt to convey my research in an effective manner at various platforms. I have received plenty of opportunities to gain scientific as well as soft skills in my thesis lab.

I am thankful to Priya for being a great support to all the students in the lab in research mentorship, experimental details and also for being a great source of encouragement throughout our thesis work.

I would especially like to thank Bharat and Ashley, my fellow graduate students and lab members for their help with experiments, feedback on paper/thesis drafts and above all their friendship, support and motivation during good and bad days.

Special thanks to my thesis committee, Drs Anthony Vella and Kamal Khanna for their constructive feedback and suggestions with the experiments. I would also like to acknowledge Drs Robert Clark and Antoine Menoret for their sound scientific advice for my research work.

I am above all thankful to my parents and my sister for their love and encouragement throughout this period. A big cheers to my friends Paurvi Shinde, Hassandeep Sidhu, Tulika Paul and Shamayeta Bhattacharya and my aunt Ms. Ahona Mukherji for their support and motivation throughout this journey.

The results of the presented work have been published in Banerjee *et al.*, 2018.

TABLE OF CONTENTS

LIST OF FIGURES

Chapter I

Introduction

A. Cytosolic DNA Sensors

The presence of DNA in the cytosol is highly immunostimulatory. A variety of host sensors recognize DNA in the cytosol. The earliest known DNA sensor is the endosomal Toll like receptor (TLR 9). TLR9 recognizes unmethylated CpG rich DNA and is highly expressed in plasmacytoid dendritic cells (pDCSs) (Ahmad-Nejad *et al*., 2000; Hemmi *et al*., 2000; Latz *et al*., 2004; Yasuda *et al*., 2009). Engagement of DNA ligand by TLR9 leads to the production of type-I IFN. Apart from the endosomal TLR9, there are many sensors that bind DNA in the cytosol. Prominent among them are AIM2 and cGAS. They bind the sugar phosphate groups in DNA therefore DNA recognition is sequence independent. While, AIM2 activation unlike other DNA sensors results in the activation and assembly of the inflammasome complex in response to DNA recognition, cGAS activation leads to the production of type-I IFN (Albrecht *et al*., 2005; Sun *et al*., 2013).

There are other DNA sensors that shuttle between the nucleus and the cytosol. Many proteins that function as a part of the DNA damage repair pathway also function as host defense sensors of DNA. The Mre11-Rasd50-Nbs (MRN) complex senses double-stranded breaks (DSBs) and also binds DNA in the cytosol in a sequence independent manner resulting in the production of type-I IFN (Kanaar *et al*.,2008; Roth *et al*, 2014). Other DNA repair proteins involved in host response to DNA include RNA Polymerase III and IFN -inducible gene 16 (IFI16) (Ablasser *et al.*, 2009; Chiu *et al.*, 2009; Kerur *et al.*, 2011; Unterholzner *et al.*, 2010).

Some RNA helicases such as DHX9, DHX36, DDX41 and DDX60 can also bind DNA and lead to type-I IFN production in response to it (Kim *et al*., 2010; Zhang *et al*., 2011 and Miyashita *et al*., 2011).

B. AIM2 and the Inflammasome complex

Inflammasomes are cytosolic multiprotein complexes that have the ability to trigger an inflammatory cascade. Members of the nucleotide-binding domain and leucine-rich repeats receptor (NLR) and absent in melanoma receptor (ALR) family are most commonly known to form inflammasome complexes. Of the NLR family NLRP1, NLRP3 and NLRC4 activation upon recognition of stimuli leads to assembly of the inflammasome complex. While in the ALR family AIM2 oligomerizes into an inflammasome macrmolecular structure in response to stimuli (Lamkanfi and Dixit.,2014). NLRs or ALRs on ligand stimulation and activation recruits a bipartite protein, apoptosis-associated speck like protein containing a caspase activation and recruitment domain (ASC) (Fernandes-Alnemri *et al*., 2007; Huang *et al*., 2009). ASC recruits caspase-1 using its CARD domain. Caspase-1 further cleaves pro-IL-1β and pro IL-18 into their mature forms that are subsequently released from the cell (Broz *et al*., 2010).

AIM2 recognizes double-stranded DNA and oligomerizes in response to it. AIM2 is part of the ALR family of proteins that contains two structural domains, the PYD domain and the HIN200 domain (Albrecht *et al*., 2005). The HIN200 domain binds DNA (Ludlow *et*

al., 2005). The PYD domain of AIM2 can recognize other PYD containing proteins. Therefore, on activation AIM2 can recruit ASC by PYD-PYD interactions (Fernandes-Alnemhri *et al*., 2009; Hornung *et al*., 2009).

A variety of microbial pathogens including viruses like mouse cytomegalovirus (MCMV), vaccinia virus and cytomegalovirus and intracellular bacteria like *Francisella tularensis, Listeria monocytogenes* and *Mycobacterium tuberculosis* can result in the activation of the AIM2 inflammasome (Jones *et al*., 2010; Rathinam *et al*., 2010; Warren *et al*., 2010). In intracellular bacterial infections pathogenic DNA can be released in the cytosol. *Francisella* can escape the phagosome and undergo baceriolysis resulting in the release of bacterial DNA in the cytosol. *Francisella* DNA activates other host DNA sensors leading to the production of type I IFN s and the up-regulation of ISGs such as IRF1. IRF1 further controls the expression of GTPases, guanylate binding proteins (GBPs) GBP 2 and 5 along with another IFN inducible protein IRGB10 induce bacterial killing (Man *et al* 2015; Man *et al*., 2016; Muenier *et al*., 2015). Mice deficient in IRGB10 and GBP along with inflammasome components AIM2 and caspase-1 have increased susceptibility to *Francisella* infections (Man *et al*., 2016).

Some pathological conditions such as cancer can result in damage to the nuclear compartment. This can result in the presentation of the nuclear material to cytoplasmic host sensors. Nuclear host DNA can thus be recognized by cytoplasmic DNA sensors cGAS and AIM2 (Di Micco *et al*., 2016). Activation of the inflammasome pathway by self-DNA can lead to the development of autoinflammatory diseases such as

polyarthritis like symptoms caused in DNase II deficient mice (Baum *et al* 2015; Jakobs *et al*., 2015).

AIM2 activation results in the recruitment of the adapter protein ASC and caspase-1. Caspase-1 proteolytically cleaves the pro-inflammatory cytokines IL-1β and IL-18 into their active forms. The activation of caspase-1 also results in the death of the cell. Caspase-1 cleaves gasdermin-D that has recently been identified as the mediator of pyroptotic cell death. Pyroptosis is a form of inflammatory cell death that results in the release of contents from the cytosol. This further triggers the excretion of proinflammatory mediators and danger signals from the cell leading to an amplification of the host immune response.

C. Gasdermin (GSDM): Activation and Pyroptosis

GSDM are a family of proteins with mice encoding 10 GSDM proteins and humans encoding 6. Gasdermin family in mice include GSDMA 1-3, GSDMC (1-4), *GSDMD*, GSDME and PJVK while the human loci encodes GSDMA, GSDMB, *GSDMD*, *GSDMD*C1, DFNA5, GSDME and PJVK. *GSDMD* has recently been identified as a substrate of inflammasome activation by three independent research groups. In their 2015 study Shi *et al* used clustered regularly interspaced short palindromic repeats (CRISPR-Cas9) system to screen for genes involved in caspase-1 and caspase-11 dependent pyroptosis. They found that mutations in *GSDMD* made the BMDMs

resistant to pyroptosis in response to inflammasome stimuli. This was accompanied by reduced IL-1β secretion by these BMDMs (Shi *et al*., 2015). Furthermore, another research group used an ethyl-nitrosourea (ENU) mutagenesis approach to study the proteins involved in caspase-11 dependent pyroptosis. They found that LPS stimulated BMDMs from mice carrying I105N mutation in *GSDMD* protein were less susceptible to caspase-11 dependent pyroptosis. Although upon prolonged treatment, *GSDMD* deficient cells eventually undergo cell death by apoptosis (Kayagaki *et al*., 2015). A third study also independently reinforced these findings (He *et al*., 2015).

GSDMD can be cleaved into its C-terminus and N-terminus domain by the inflammatory caspases-1,4.5 and 11(He *et al*., 2015; Kayagaki *et al*., 2015; Shi *et al*., 2015). *GSDMD* N-terminus can bind to lipids in the plasma membrane. It can bind to phosphatidyl inositol phosphates (PIPs) such as PI4P, PI(4,5)P2, PI3P and PI5P(Ding *et al*., 2016; Liu *et al*., 2016). However *GSDMD* N-terminus cannot bind to phosphatidyl ethanolamine and phosphatidyl choline that are prominent in the outer surface of the plasma membrane lipid bilayer (Liu *et al*., 2016). This prevents the death of bystander cells in an inflammatory environment. Interestingly *GSDMD* binds cardiolipin on the bacterial outer membrane (Liu *et al*., 2016). This results in the lysis and killing of bacteria such as *Escherichia coli*, *Staphylococcus aureus* and *Listeria monocytogens* (Liu *et al*., 2016).

The size of the *GSDMD* pore formed is 10 -16 nm wide. The pore is non-selective and molecules with a smaller size can be released through the pore while higher molecular size proteins are restricted.

The active forms of pro-inflammatory cytokines such as IL-1β and IL-18 have a molecular size of 4 nm and are hence released through the *GSDMD* pore (Ding *et al*., 2016 and Liu *et al*., 2016). Lactate dehydrogenase (LDH) on the other hand is a tetrameric molecule with a molecular size of 10 nm and is restricted (Evavold *et al*., 2018). Whether cells that have a certain threshold of *GSDMD* pores proceed towards pyroptosis requires further investigation in the field.

GSDMD is associated with functions apart from its role in cell death. The release of caspase-1 cleaved mature IL-1β and IL-18 from the cell in the absence of cell lysis was shown prior to the discovery of *GSDMD* in 2006 (Fink and Cookson, 2006). A recent study further corroborated this by demonstrating the role of *GSDMD* pores in the release of IL-1β in the absence of cell lysis (Evavold *et al*., 2018). The study uses an osmoprotectant glycine that blocks cell lysis measured by LDH release but allows the formation of *GSDMD* pores assessed by the entry of propidium iodide in the cell. On treatment of primary macrophages with inflammasome activating stimuli, bioactive IL-1β is released through the *GSDMD* pores even though glycine treatment blocks cell lysis and LDH release. Furthermore, treatment with stimuli that do not cause pyroptosis but lead to inflammasome dependent gasdermin-D activation and pore formation such as bacterial peptidoglycan, the peptidoglycan component N-acetyl glucosamine (NAG), *S. aureus* O-acetyl transferase A (Oat A) mutant leads to IL-1β release through the

GSDMD pores in the absence of cell lysis (Evavold *et al*., 2018). A similar phenotype is observed in other myeloid cell types such as primary dendritic cells (DCs). In bone marrow derived dendritic cells (BMDCs), treatment with oxidized phospholipids (OxPAPC) results in the release of IL-1β in the absence of pyroptosis (Hellig *et al*., 2018). These studies demonstrate the role of gasdermin-D in secretion of bioactive pro-inflammatory cytokines in viable cells.

These studies however fail to establish the kinetics of cytokine release and cell death. More investigation is required to establish the sequential events leading to pyroptosis. Prolonging this window period between the formation of *GSDMD* pore formation and the lysis of the cell leads to the enhanced release of inflammatory mediators from the cell and also results in increased T cell priming and antigen-specific response (Gong *et al*., 2017; Zamoin *et al*., 2016). Recent studies have also shown that IL-1β can be released from the cell in a *GSDMD* dependent or independent manner. The early release of IL-1β in inflammasome activated non-pyroptotic cells is dependent on *GSDMD* secretion at later stages is independent of it (Monteleone *et al*., 2018; Schneider *et al*., 2017). Neutrophils express *GSDMD* to a lesser extent than macrophages and dendritic cells and can release cleaved IL-1β even from *GSDMD* lacking neutrophils (Hellig *et al*., 2018).

Apart from its role in the secretion of cytokines *GSDMD* is also essential for the formation of neutrophil extracellular traps (NETs) against extracellular microbes. NETS are composed of chromatin and anti-microbial compounds. On the recognition of LPS

from extracellular gram-negative bacteria by neutrophils the non-canonical inflammasome signaling is activated resulting in the activation and cleavage of caspase-11 and *GSDMD*. The activation of *GSDMD* in neutrophils is indispensable to the formation of NETs. *GSDMD* is required in mediating the early events in the formation of NETs such as nuclear membrane disruption and histone degradation that results in nuclear expansion along with the final stage events such as cell lysis and NET extrusion (Chen *et al*., 2018; Sollberger *et al*., 2018). Blocking the formation of NETs by deoxyribonuclease–I treatment in *Salmonella* sifA mutant infection that stimulates the caspase-11 inflammasome by its LPS, leads to higher bacterial burdens in wild type mice. However, a similar phenotype is not seen with Casp-$11^{-/-}$ and $GSDMD^{-/-}$ mice (Chen *et al*., 2018).

D. Other Gasdermin family members

GSDMA

GSDMA, has been the most studied GSDM family protein after *GSDMD*. It is encoded as a single protein GSDMA in the human genome while the mouse genome encodes three proteins GSDMA 1-3. GSDMA has a structure similar to *GSDMD*. It has an N and a C-terminus domain, with the N-terminus being auto-inhibited by the C-terminus. Due to its structural similarity with *GSDMD*, it was predicted that GSDMA could also form membrane pores. When over-expressed in 293T cells GSDMA and GSDMA3 can form pores in the plasma membrane and result in cell lysis by pyroptosis, thereby causing

cytotoxicity (Ding *et al*., 2016). Although, this has not been reported thus far in a physiological system. However, GSDMA has been shown to form pores in the mitochondrial membrane (Lin *et al*., 2015; Shi *et al*., 2015). The N-terminal domain of GSDMA3 can interact with and inhibit TRAP1, a mitochondrial chaperone that aids in reducing mitochondrial permeability and apoptosis (Shi *et al*., 2015).

Mutations in GSDMA that results in the release of N-terminus inhibition are associated with a variety of disease phenotypes such as alopecia, cutaneous inflammation, heightened immune responses and enlarged spleen, hyperplasia (Ding *et al*., 2016; Guo *et al*., 2017; Kumar *et al*., 2012; Wood *et al*., 2005; Zhou *et al*., 2012). The Y344H mutation that abrogates the N-terminus auto-inhibition has been investigated in some depth. The Y344H mutation is associated with the previously described phenotype of enlarged lymph nodes and aggressive immune responses (Guo *et al*., 2017; Wood *et al*., 2005). This mutation in GSDMA3 is associated with a decrease in caspase-3 expression thereby leading to reduced apoptosis in keratinocytes (Lei *et al*., 2012). Also, the Y344H mutation leads to the reduction in mitochondrial membrane potential and increased reactive oxygen species (ROS) generation (Shi *et al*., 2015).

GSDMB

In contrast to the other members of the gasdermin family GSDMB is carried by humans but not mice (Runkel *et al*., 2004). GSDMB also differs from other family members due to its membrane binding ability. The N-terminus as well as the full-length GSDMB protein can bind to membrane lipids such as phosphoinositides and glycolipids (Chao *et*

al., 2017). However only the N-terminal GSDMB fragment can form poresin the plasma membrane and induce pyroptosis (Ding *et al*., 2016). The cleavage of GSDMB is controversial. One study reports the cleavage of GSDMB by apoptotic caspases-3 and 7 instead of caspase-1, 4 or 5 (Chao *et al*., 2017). While another contrasting group has demonstrated the cleavage of GSDMB by inflammatory caspase-1 (Panganiban *et al*., 2018). Although the later study uses overexpression of GSDMB and caspase-1 in HEK 293T cells as their model system and this may not be an accurate measure of physiological conditions. GSDMB gene is associated with various inflammatory disease phenotypes. The most prominent being inflammatory bowel disease, type-I diabetes and asthma (Halapi *et al*., 2010; Kang *et al*., 2012; Li *et al*., 2012; Mofatt *et al*., 2010; Wu *et al*., 2009).

GSDMC

Although GSDMC N-terminal fragment like other GSDM family proteins can form pores and induce pyroptosis on overexpression in 293Ts, GSDMC has not been reported to be cleaved by caspases in a physiological environment (Ding *et al*., 2016). Some studies have demonstrated its ability to serve as a transcription factor. It has a leucine zipper motif in its structure that suggests DNA binding ability (Watabe *et al*., 2001).

GSDME/DFNA5

GSDME is most widely studied for its association with hearing impairment in humans. Mutant GSDME protein resulting in a truncated C-terminus is strongly correlated with this phenotype. Contrary to other family members GSDME is cleaved by caspase-3, an

apoptotic effector caspase. On cleavage by caspase-3 GSDME can form pores in the plasma membrane and induce pyroptosis (Rogers *et al*., 2017; Wang *et al*., 2017).

PJVK/DFNB59

PVJK (DFNB59) similar to GSDME is associated with impaired cochlear responses in humans and mice. Mutations in PJVK can lead to nonsyndromic recessive deafness in human patients (Delmaghani *et al*., 2006; Delmaghani *et al*., 2015).

E. c-GAS/STING Signaling

Pathogen invasion and release of microbial DNA in the cytosol results in the activation of host DNA sensors in the cytosol. Another sensor that detects DNA in the cytosol along with AIM2 is cGAS. Apart from microbial DNA, self-DNA can also enter the cytoplasm under pathological conditions and in a tumor microenvironment. This can also be recognized by cytosolic DNA sensors such as cGAS.

cGAS contains a DNA-binding domain and a catalytic nucleotidyltransferase domain (Sun *et al*., 2013). On binding DNA using its DNA-binding domain cGAS undergoes dimerization (Li *et al*., 2013 and Zhang *et al*., 2014). cGAS recognizes double stranded (ds) DNA in a sequence-independent manner (Sun *et al*., 2013). B-form of DNA can optimally bind cGAS as it has the ability to push an activation loop in the active site of cGAS resulting in its activation (Zhang *et al*., 2014). DNA binding to cGAS induced a

structural change that results in the synthesis of a secondary messenger cyclic GMP-AMP (cGAMP), a dinucleotide from its substrates GTP and ATP (Sun *et al*., 2013, Zhang *et al*., 2014, Li *et al*., 2013 and Wu *et al*., 2013). 2'3'cGAMP binds to STING, an adaptor localized in the endoplasmic reticulum (ER) membrane and induces its dimerization (Ishikawa *et al*., 2008; Wu *et al*., 2013; Zhang *et al*., 2013; Zhong *et al*., 2008). STING traffics from the ER to the golgi apparatus (Doobs *et al*., 2015; Ishikawa *et al*., 2009; Saitoh *et al*., 2009). STING activation and dimerization further results in auto-phosphorylation of the kinase TBK-1. TBK-1 phosphorylates IRF3 that subsequently dimerizes and enters the nucleus. IKK is also activated during STING signaling. IKK activation results in the release of NF-κB from inhibition. IRF3 and NF-κB are recruited to the nucleus where they result in the transcription of IFN-α/β and pro-inflammatory cytokines such as tumor necrosis factor (TNF) and IL-6 respectively (Fitzgerald *et al*., 2003; Ishikawa *et al*., 2008; Sharma *et al*., 2003; Tanaka *et al*., 2012).

F. Regulation of cGAS/STING Signaling

Regulation of cGAS

cGAS can be regulated by a variety of mechanisms prominent among them are regulation of cGAS through post-translational modifications. Glutamylation of cGAS is an important regulator of its catalytic activity. Glutamylases TTLL4 and TTLL6 are responsible for glutamylation of cGAS while deglutamylation enzymes CCP5and CCP6 reverse the modification. Glutamylation of cGAS inhibits its activity. It has been

postulated that at steady state there is maintenance of homeostasis between glutamylated and deglutamylated cGAS (Xia *et al*., 2016). Akt can regulate cGAS activity by phosphorylation of a serine residue. Akt can phosphorylate Ser291 in mouse and Ser 305 in human cGAS.

Recent evidences in literature have uncovered the cross-talk between inflammasome activation and type-I IFN production. Corrales *et al*., 2016 described what had been previously observed by various groups (Fernandes-Alnemri *et al*., 2010; Gray *et al*., 2016; Hornung *et al*., 2009; Jones *et al*; 2010; Rathinam *et al*; 2010) that AIM2 inflammasome regulates cGAS/STING mediated type-I IFN production. However, their study lacked the mechanistic insights of this process. Another study showed that caspase-1 when activated in DNA virus infection can cleave cGAS and thus regulates type-I IFN production (Wang *et al*., 2017).

Regulation of STING

Similar to cGAS post-translational modifications can also regulate STING. Phosphorylation of STING at Ser366 leads to the degradation of STING and suppression of type-I IFN production (Konno *et al*., 2013). Ubiquitination is another post-translational modification capable of regulating STING. E3 ubiquitin ligase TRIM56 and TRIM32 are reported to enhance the Lys (K) 63 polyubiquitination of STING. Thereby, enhancing type-I IFN productin (Tuchida *et al*., 2010; Zhang *et al*., 2012). However, the role of ubiquitination is considered controversial. The E3 ligase complex containing

AMFR, GP78 and INSIG1 promote K63 ubiquitination and promote STING function (Wang *et al*., 2014). However, the E3 ligase complex containing RNF5 and TRIM30a promote K48 ubiquitination instead and target STING for degradation (Wang *et al*., 2015; Zhong *et al*., 2014).

cGAS-dependent type-I IFN production can also be regulated by influencing the stability and transport of the secondary messenger cGAMP. ENPP1, an enzyme present in the extracellular milieu has been reported to degrade cGAMP (Li *et al*., 2014).

F.Type-I IFN Signaling

Both human and murine type-I IFN family consists of 16 proteins; 12 IFN-α, IFN-β, IFN-ε, IFN-κ, IFN-ω (McNab *et al*., 2015). Type-I IFNs can bind to the heterodimer receptor IFNAR-1 and IFNAR-2, thus initiating a downstream cascade of events. Binding to the IFNAR receptor leads to the phosphorylation and activation of Janus-associated kinase (JAK)-1 and tyrosine kinase (TYK)-2 (Plaintainas *et al*., 2005). Resulting in the phosphorylation of STAT1 and STAT2 that enables it to dimerize and recruit IRF9. STATI-STAT2-IRF9 complex then translocates to the nucleus where it binds to IFN response element (ISRE). To activate the transcription of IFN stimulated genes (ISGs) (Stark and Darnell Jr., 2012). Mitogen activated protein kinase (MAPKs) such as p38 and ERK can also play a role in ISG expression (Platainias *et al*., 2005). ISGs affect a variety of cellular functions such as proliferation, differentiation, apoptosis and innate immune response to pathogens.

Heightened type I IFN response due to a failure of its regulatory mechanisms can lead to various chronic auto-immune and inflammatory diseases. Auto-immune diseases such as rheumatoid arthritis, systemic lupus erythematosus (SLE), Sjogen's syndrome and Systemic sclerosis display the IFN signature (Hall and Rosen, 2010). Type-I IFN is crucial for the pathogenesis of SLE. There is increased expression of ISGs in lupus patients (Kalliolas and Ivashikiv, 2010). IFN receptor (IFNAR) deficient mice displayed a lack of lupus-specific autoantibodies (Nacionales *et al*., 2007). Enhanced IFN-α production from plasmacytoid dendritic cells (DCs) of SLE patients further emphasized the role of type I IFN in SLE (Henault *et al*., 2016).

H. Francisella Pathogenesis

Francisella tularensis is a facultative intracellular gram-negative bacterium and the causative agent of tularemia. It primarily resides in macrophages although it has been shown to infect other myeloid cells such as dendritic cells and neutrophils and non-immune cells such as alveolar epithelial cells and hepatocytes (Hall *et al*., 2007; Long *et al*., 1993; McCaffrey and Allen, 2006). *Francisella tularensis* subsp. *novicida*, a murine pathogen has been extensively studied to investigate the mechanistic aspects of *Francisella* pathogenesis. *F. novicida* is taken up by macrophages in a phagosome. The phagosome initially fuses with the early endosome and then gets converted into the late endosome. At this stage on further acidification of the phagosomal compartment *F. novicida* escapes into the cytosol and replicates (Clemens *et al*., 2004, Santic *et al*.,

2005). Bacterial virulence factors grouped into the *Francisella* pathogenicity island (FPI) locus are indispensible for the release of the pathogen into the cytoplasm (Nano *et al*., 2004). FPI mutant *F. novicida* cannot escape the phagosome and is ultimately degraded by the fusion of the phagosome to the lysosome and is therefore not infectious (Bonquist *et al*.,2008, Brotcke *et al*., 2006 and Weiss *et al*., 2007). *F. novicida* can be detected by host defense sensors in the macrophages. LPS from *F. novicida* is structurally different from other gram-negative bacterial pathogens. Lipid A of *F. novicida* LPS is tetra-aceylated and is therefore not recognized by TLR4 that optimally recognizes hexa-aceylated LPS (Barker *et al*., 2006; Cole *et al*., 2006; Hajjar *et al*., 2006; Raetz *et al*., 2009). *F. novicida* can however be recognized by TLR2 but only in an intranasal challenge (Collazo *et al*., 2006; Malik *et al*., 2006).

I. Francisella recognition in the cytosol

F. novicida escapes the phagosome and enters the cytoplasm, this makes it recognizable by the cytosolic host defense sensors thereby allowing the host to mount an immune response against the bug. The first indication of the cytosolic host response came from the study describing the role of IFN signaling in *F. novicida* infection (Henry *et al*., 2007). Thereafter it was thought that the IFN -inducible AIM2 plays a role in *F. novicida* recognition. In macrophages from AIM2 deficient mice there was an absence of inflammasome response to *F. novicida* demonstrating the role of AIM2 in inflammasome activation in response to *F. novicida* (Fernandes-Alnemri *et al*., 2010; Jones *et al*., 2010; Rathinam *et al*., 2010). AIM2 inflammasome activation is critical for

the host response to *Francisella* infection. AIM2 deficient mice have higher bacterial burdens and succumb to infection earlier than their wild type counterparts (Fernandes-Alnemri *et al*., 2010; Jones *et al*., 2010).

F. novicida is also recognized by other cytosolic host sensors. As previously mentioned *F. novicida* infection elicits a IFN response in macrophages (Henry *et al*., 2007). In subsequent studies, it was shown that stimulator of interferon genes (STING) is required for IFN response to *F. novicida* infection (Jin *et al*., 2011; Jones *et al*., 2010; Peng *et al* 2011). Type I IFN signaling in *F. novicida* infection drives the expression of IFN -inducible guanylate binding proteins (GBPs) especially GPB2 and GBP5 that are recruited to the bacterial surface. GBP2 and 5 are instrumental in bacterial lysis and release of DNA in the cytosol (Man *et al*., 2015 and Muenier *et al*., 2015). This bacterial DNA is then bound by the cytosolic DNA sensor AIM2 leading to inflammasome assembly and activation (Fernandes-Alnemri *et al*., 2010; Jones *et al*., 2010; Rathinam *et al*., 2010). GBP 2 and 5 are required to activate the AIM2 inflammasome and mice deficient in these proteins succumb to a *Francisella* challenge earlier than wild type mice (Man *et al*., 2015; Muenier *et al*., 2015).

Since STING is required for IFN response to *F. novicida* infection (Jin *et al*., 2011, Jones *et al*., 2010; Peng *et al* 2011), the cytosolic DNA sensor that recognizes *F. novicida* DNA and elicits Type I IFN production could be cGAS. Storek *et al* subsequently found cGAS and Ifi204 to be cytosolic sensors of *F. novicida* DNA (Storek *et al*., 2011).

J. Francisella and Type I IFN

The role of type-I IFN in bacterial infection varies depending on the nature of the bacterial pathogen. In *Streptococcus* infections type-I IFN plays a protective role (McNab *et al*., 2015). While in *Mycobacterium tuberculosis*, *Listeria monocytogenes* and *F. novicida* infections it is harmful for the host (Auerbuch *et al*., 2004, Henry *et al*., 2010, Mayer-Barber *et al*., 2014, McNab *et al*., 2015 and Storek *et al*., 2015). A recent study shows that although type-I IFN produced by cGAS/STING signaling has a crucial role in activating the AIM2 inflammasome (Man *et al*., 2017), it has an overall detrimental role in *F. novicida* infection. The authors show that IFN receptor Ifnar1 or Ifnar2 deficient and Ifnar2 AIM2 double deficient mice are more susceptible to *F. novicida* infection than their wild type counterparts. They further report increased apoptosis due to type-I IFN signaling in the liver in *F. novicida* infection. This may explain the detrimental role of IFN signaling as it has been previously demonstrated that hepatocytes have an essential role in *F. novicida* infection (Zhou *et al*., 2016 and Zhu *et al*., 2018). Some immune cell types such as $\gamma\delta$ T cells may undergo less cell death in the absence of type-I IFN signaling and thereby they might secrete increased levels of protective IL-17 and IL-12 in *F. novicida* infection (Zhu *et al*., 2018).

Chapter II

Materials and Methods

Results of the presented work have been published in Banerjee *et al*., 2018.

A. Experimental Models

Mice C57BL/6J, Casp1/11$^{-/-}$, AIM2$^{-/-}$, Il1r$^{-/-}$, and Il18r$^{-/-}$ mice obtained from the Jackson Laboratory (Bar Harbor, ME) were bred and maintained in specific pathogen–free conditions in the animal facilities of UConn Health. GSDMD$^{-/-}$ (Kayagaki *et al*., 2015), AIM2$^{-/-}$ (Jones *et al*., 2010), and caspase-11$^{-/-}$ mice (Kayagaki *et al*., 2011) obtained from Genentech (South San Francisco, CA) were also bred and maintained in specific pathogen–free conditions in the animal facilities of UConn Health. Asc$^{-/-}$ (Rathinam *et al*., 2010), Nlrp3$^{-/-}$ (Rathinam *et al*., 2012), cGas$^{-/-}$ (Suschak *et al*., 2016) mice were described previously. Both male and female mice of 8-24 weeks old were used. The animal protocols were carried out in accordance with the guidelines set forth by the UConn Health Institutional Animal Care and Use Committee.

Differentiation of primary Bone-marrow Derived Macrophages

Primary bone-marrow derived macrophages (BMDMs) were generated by culturing bone marrow cells from wild-type and various knockout mice in DMEM with 10% FBS and 20% L929 supernatants for 8 to 12 days. Cell culture media was replaced on day 3 with fresh DMEM with 10% FBS and 20% L929 supernatants. Cells were harvested and used for experiments between days 7 and 12 of culture.

Bacterial Strains

Bacteria and viruses used in this study include *Francisella tularensis* subsp. *novicida* strain Utah 112 (*F. novicida*; BEI resources, NIAID, NIH), Enterohemorrhagic *E. coli* (Vanaja *et al*., 2016), *E. coli* BL21 (Vanaja *et al*., 2016), and Sendai virus (Cantrell strain; Charles River Laboratories).

B. Methods

Cell stimulations and Infections

F. novicida was grown over night at 37°C in Mueller Hinton broth. BMDMs and RAW macrophages were infected at an MOI of 50 or 100 (unless otherwise indicated) and after 1 – 2 h of infection, medium was replaced with gentamicin (100 mg/ml) containing medium. Cells were infected with Sendai virus (15 HA units/ml). Cells were transfected with lipofectamine 2000 (2 ml/ml) complexed poly(dA:dT) (1 µg/106 cells) or 2'-3'-cGAMP (2.5 µg/106 cells) and stimulated with poly(I:C) (25 µg/ml), LPS (1 µg/ml). Supernatants were collected 6 h post-stimulations unless otherwise indicated. In certain experiments, cells were primed with 400 ng/ml Pam3CSK4 for 2–3 h before stimulations to assess inflammasome responses. The supernatants were collected 6–8 h post-stimulation unless otherwise indicated. In some experiments, glycine (50 mM) was added to cells at the time of or 1 h after stimulations. In experiments where K^+ efflux was inhibited, increasing concentrations of KCl was added to the medium at the time of stimulations. In experiments where K^+ efflux was induced, cells were treated with

nigericin or valinomycin at the indicated concentrations 1.5-2 h after the stimulations or were incubated in K^+ free medium throughout the duration of the experiment. Further, in some media replacement experiments, nigericin-containing media was replaced with DMEM without nigericin 1 h post addition of nigericin. Inhibition or induction of K^+ Efflux using isosmotic media Isosmotic medium without or with defined concentrations of KCl was prepared as described previously (Rühl and Broz, 2015). Cells were infected with *F. novicida* and after 1 h of infection medium was replaced with gentamicin (100 mg/ml) containing buffer A (4.2 mM Na2CO3, 0.8 mM Na2HPO4, 1.3 mM CaCl2, 0.5 mM MgCl2, 10 mM D-glucose monohydrate, pH 7.4). For K^+ efflux inhibition, cells were incubated in buffer A supplemented with 137 mM NaCl and 5 mM KCl, 117 mM NaCl and 25 mM KCl, or 92 mM NaCl and 50 mM KCl. For K^+ efflux induction, cells were incubated in buffer A supplemented with 142 mM NaCl but without KCl. Cells were then stimulated and supernatants were collected as described above. Additionally, in some experiments 5 mM (iso-osmotic concentration) KCl was added to K^+ free media 1 h post exposure to K^+ free media.

ELISA, Cell Death Assay, and Immunoblotting

Levels of IFN-β and IL-18 in culture supernatants or plasma were assessed by ELISA as described before (Bossaller *et al*., 2012; Roberts *et al*., 2007). IFN-β levels are presented as units/ml or pg/ml depending upon the recombinant IFN-β standard used in the ELISA. IL-1β and IL-6 levels were assessed by Ready-Set-Go!® ELISA kits (eBioscience) according to the manufacturer's instructions.

Cell death was assessed by LDH cytotoxicity detection kit (Clontech) unless otherwise indicated according to the manufacturer's instructions. Intracellular ATP and metabolic activity was measured by using CellTiter-Glo assay (Promega) and PrestoBlue assay (Invitrogen), respectively, according to the manufacturer's instructions.

For western analysis, cells were lysed with 1% NP-40 lysis buffer. Samples were run on 12.5% polyacrylamide gels and transferred onto nitrocelluose membranes by using Trans-Blot Turbo Transfer System (Bio-Rad). Blots were then blocked and probed with appropriate primary and secondary antibodies, and proteins bands were visualized with Bio-Rad Clarity ECL HRP substrate on a Syngene gel documentation box.

Liquid Chromatography-Mass Spectrometric measurement of cGAMP

Cells were stimulated with *F. novicida* or poly(dA:dT) for 5 h and snap-frozen. Cell extract prepared with methanol was filtered with 30 kDa filter to remove debris, dried, resuspended in water. c-di-AMP was added to the samples as an internal control. Samples were transferred to vials, capped and placed into the autosampler (kept at 4 °C). Aliquots of 10 or 20 µl from each vial was injected, along with cGAMP standards, onto the LC–MS/MS system (Agilent 1200 Autosampler and Binary pump 20 (Wilmington, DE, USA) coupled to an ABI4000Q bench top mass spectrometer (MDS SCIEX, Concord, ON, Canada). The MRM m/z transitions monitored for cGAMP and c-di-AMP were 675.5>506.0, and 659.0>524.0, respectively. Data was collected with the

Analyst software.

Intracellular Potassium Measurement

Wild-type, GSDMD$^{-/-}$, caspase-1/11$^{-/-}$, and AIM2$^{-/-}$ cells plated in 96-well clear bottom black plates were stimulated with *F. novicida* in glycine (50 mM)-containing media. After 6 h of stimulation, medium was replaced with PBS containing asante potassium green (APG)4 for 1 h, which is extremely specific for K^+ (Eil *et al*., 2016; Prindle *et al*., 2015), and pluronic acid F-127, which aids in efficient permeation of APG4 into the cells. After 1 h of incubation at 37°C, cells were washed with PBS and the fluorescence was read with ClarioStar multimode microplate reader (BMG LABTECH, Germany).

Reconstitution of GSDMD$^{-/-}$ iBMDMs with GSDMD

HEK293T cells were transfected with pMSCV-puro (empty vector; EV), pMSCV-puro encoding 2xFLAG-HA-GSDMD, or pMSCV-puro encoding 2xFLAG-HA-I105N GSDMD mutant and retro viral packaging plasmids. Viral supernatants collected after 48 and 72 h of transfection were concentrated by centrifugation at 20,000 x g for 2 h and used to transduce GSDMD$^{-/-}$ iBMDMs. Transduced cells were selected using puromycin, and the expression of wild-type and mutant GSDMD was verified by western blotting with FLAG and GSDMD antibodies.

Mice Infections

F. novicida was grown over night at 37°C in Mueller Hinton broth. C57BL/6 (wild-type; WT), AIM2-deficient (Rathinam *et al*., 2010), caspase-1/11$^{-/-}$, and GSDMD$^{-/-}$ mice were subcutaneously infected with 1.5 or 5 Å~ 105 CFU of *F. novicida*. Cytokine levels in the plasma were analyzed at 24 h post-infection. C57BL/6 (wild-type; WT) and AIM2$^{-/-}$ mice were infected with 1 Å~ 109 CFU of E. coli BL21 by i.p. injection. Cytokine levels in the plasma were analyzed at 6 h post-infection. Mice were infected with 2.5 Å~ 102 CFU of *F. novicida* in the survival studies. In some survival experiments, WT and AIM2$^{-/-}$ mice were injected i.p. with 250 mg of an isotype control or anti-IFNAR antibody (clone: MAR1-5A3) 12 h p.i.

cGAS-DNA binding assay

Wild-type and *GSDMD*$^{-/-}$ BMDMs were stimulated with *F. novicida*. After 6 h post stimulation, media was replaced with PBS containing 1% paraformaldehyde (PFA), and the cells were incubated for 10 min at room temperature. The crosslinking reaction was then quenched with 0.1 M Tris pH 7.4 in PBS. The cells were the collected and lysed in 0.5%Triton-X 100 lysis buffer. cGAS immunoprecipitation was performed by adding protein A beads and anti- cGAS antibody to the lysates After overnight incubation at 4 C, beads were washed twice with low salt, high salt, and lysis buffers. Then antibody/protein/DNA complexes were eluted with a freshly prepared elution buffer (1% SDS/0.1 M NaHCO3 pH 8.0) Beads mixed with elution buffer was shaken on vortex for 15 min and then centrifuged at 13,000 rpm for 3 min. Eluted samples were then de-crosslinked by adding 0.3 M sodium chloride and incubating at 65 C for 4h. This was

followed by protein digestion using proteinase K at 45 C for 2 h. DNA was finally purified using phenol/chloroform/isoamyl alcohol precipitation. *F. novicida* DNA bound to cGAS was quantified by real time PCR with primers targeting bacterial genome (mglA), The PCR products were also run on a 1.5% agarose gel and imaged under UV light using a Syngene gel documentation box.

cGAS Immunofluorescence Staining

Wild-type and GSDMD$^{-/-}$ BMDMs were infected with *F. novicida* or transfected poly(dA:dT). After 5 h, the cells were washed with PBS, fixed with 4% paraformaldehyde, permeabilized with 0.1% Triton-X, blocked with 10% goat serum, incubated overnight at 4 oC with anti-cGAS antibody, and stained for 1 h with fluorescently labeled anti-rabbit secondary antibody. Plasma membrane and nucleus/DNA were stained with cholera toxin B Alexa fluor 647 conjugate (CTB) (Life Technologies) and DAPI, respectively. The cells were visualized using a Zeiss LSM 780 microscope.

In vitro cGAS Enzymatic Assay

Recombinant mouse cGAS (catalytic domain) (28 ng) was mixed in a 10 ml reaction buffer (20 mM Tris-Cl [pH 7.4], 5 mM MgAc) with 10 or 2 ng DNA (100 base pair), 12 mM each ATP and GTP, and 5.0 mCi of a-32P-ATP (800Ci/mmol). After 120 min of incubation at 37 °C, the reaction mixture was heated to 65 °C for 5 min, treated with

calf-intestinal alkaline phosphatase, and analyzed by thin layer chromatography (TLC) as described before (Kranzusch *et al*., 2013).

Flow Cytometry

For flow cytometric quantification of viperin expression, cells were stimulated with *F. novicida*, poly(dA:dT), or IFN-β (500 IU/ml) for 16 h. Cells were fixed in 4% paraformaldehyde and permeabilized with 0.1% saponin in PBS and stained with anti-viperin antibody in FACS buffer (PBS with 3%FBS and 0.1% sodium azide). Samples were run on LSR-II (BD Biosciences) and analyzed using FlowJo software.

Quantification and Statistical Analysis

Data were analyzed for statistical significance by two-way ANOVA followed by the Sidak's post- test, unpaired two-tailed t test, or Mantel-Cox test as indicated with Prism Software. *, $P < 0.05$; ns, not significant.

Chapter III

Results

Results of the presented work have been published in Banerjee *et al*., 2018.

A. AIM2 inflammasome inhibits IFN-β response to cytosolic DNA in vitro and in vivo

F. novicida is a cytosolic pathogen that robustly activates IFN-β response via its DNA (Fernandes-Alnemri *et al*., 2010; Jones *et al*., 2010; Man *et al*., 2015a; Meunier *et al*., 2015; Rathinam *et al*., 2010; Storek *et al*., 2015) and thus represents a valuable model system to investigate cGAS regulatory mechanisms in bacterial infections. *F. novicida* also stimulates another cytosolic DNA receptor, AIM2 (Fernandes-Alnemri *et al*., 2009; Hornung *et al*., 2009; Jones *et al*., 2010; Man *et al*., 2015a; Meunier *et al*., 2015; Rathinam *et al*., 2010). In contrast to cGAS that induces transcriptional induction of the type I IFN, AIM2, upon directly binding DNA in the cytosol, forms an inflammasome complex by oligomerizing ASC and caspase-1. Infection with *F. novicida* or transfection of the synthetic double stranded DNA mimetic, poly(dA:dT), into the cytosol induced IL-1β secretion in wild-type bone marrow derived macrophages (BMDMs), and this response was abolished in AIM2$^{-/-}$ BMDMs (Fig. 1A). In stark contrast, AIM2$^{-/-}$ BMDMs secreted higher levels of IFN-β than wild- type BMDMs in response to *F. novicida* (Fig. 1B). Similarly, poly(dA:dT)-induced IFN-β secretion was elevated in AIM2$^{-/-}$ BMDMs compared to wild-type BMDMs consistent with the earlier observations (Fig. 1B) (Corrales *et al*., 2016; Fernandes-Alnemri *et al*., 2010; Gray *et al*., 2016; Hornung *et al*., 2009; Jones *et al*., 2010; Rathinam *et al*., 2010). In line with their enhanced production of IFN-β, *F. novicida*- and poly(dA:dT)-stimulated AIM2$^{-/-}$ BMDMs, compared to wild-

type BMDMs, expressed higher levels of IFN stimulated gene (ISG) products such as viperin and ISG15 (Fig. 1C). AIM2 has been shown to inhibit colon tumorigenesis independently of the inflammasome complex (Man *et al*., 2015b; Wilson *et al*., 2015). To test if the IFN-suppressive role of AIM2 is inflammasome-dependent or - independent, we used $Asc^{-/-}$ and caspase-$1/11^{-/-}$ macrophages. ASC-, and caspase-1/11- deficient BMDMs phenocopied AIM2-deficient BMDMs and produced more IFN-β after poly(dA:dT) transfection or *F. novicida* infection (Fig. 1D and 1E). Moreover, unlike poly(dA:dT) and *F. novicida*, TLR ligands (LPS and poly(I:C)) and RNA virus (Sendai) that do not engage the AIM2 inflammasome induced normal levels of IFN-β production in $AIM2^{-/-}$, $Asc^{-/-}$, or caspase- $1/11^{-/-}$ BMDMs (Fig. 1D-F). Taken together, these data clearly demonstrate that AIM2-mediated inhibition of IFN- β is dependent on its inflammasome-activating ability (Corrales *et al*., 2016; Wang *et al*., 2017). We examined if AIM2 exhibits a similar suppressive effect on cGAS-induced IFN-β response to cytosolic DNA during bacterial infections in vivo. Towards this end, we utilized the *F. novicida* infection model as *F. novicida* stimulates both cGAS-STING-IFN-β and AIM2 inflammasome pathways in mice (Fernandes-Alnemri *et al*., 2010; Jones *et al*., 2010; Man *et al*., 2015a; Meunier *et al*., 2015; Rathinam *et al*., 2010; Storek *et al*., 2015). In line with the in vitro results in macrophages, plasma IFN-β levels at 24 h p.i were significantly higher in *F. novicida*- infected mice lacking AIM2 than in infected wild-type mice (Fig. 1G). On the other hand, wild- type mice had increased levels of IL-1β in plasma compared to $AIM2^{-/-}$ mice (Fig. 1H). We further tested the involvement of the inflammasome complex in AIM2 suppression of cGAS signaling by monitoring *F. novicida*-induced IFN- β production in caspase-$1/11^{-/-}$ mice. Similar to our observations

in AIM2$^{-/-}$ mice, caspase-1/11$^{-/-}$ mice had significantly elevated levels of IFN-β but reduced levels of IL-18 in plasma relative to wild-type mice (Fig. 1I and 1J). Furthermore, *E. coli*, which engages the caspase-11-noncanonical inflammasome but not the AIM2 inflammasome (Kailasan Vanaja *et al*., 2014; Rathinam *et al*., 2012), induced comparable levels of IFN-β production in wild-type and AIM2$^{-/-}$ mice (Fig. 1K). Thus, it is evident from all these data that the AIM2 inflammasome functions to limit cytosolic DNA-induced type I IFN responses *in-vivo*.

B. AIM2 restricts cytosolic DNA-driven type I IFN responses via GSDMD

GSDMD is a newly identified substrate for inflammasome-activated caspase-1 (He *et al*., 2015; Kayagaki *et al*., 2015; Shi *et al*., 2015). This raises two possibilities by which the AIM2 inflammasome may exert its regulatory effect on IFN-β production; first, caspase-1 activated by AIM2 may directly regulate cGAS-induced IFN-β production without involving GSDMD. Consistent with this possibility, a recent study showed that, during viral infections, caspase-1 depletes cellular levels of full length cGAS by cleaving it and thus inhibiting type I IFN production (Wang *et al*., 2017). However, in our study, strong caspase-1 activation by AIM2 inflammasome ligands, *F. novicida* and poly(dA:dT), and NLRP3 stimuli, nigericin and ATP, in wild-type BMDMs did not result in any reduction in cGAS protein levels or its cleavage (Fig. 2A). An alternative possibility is that GSDMD activated by the AIM2 inflammasome (Fig. S1A) (Kayagaki *et al*., 2015;

Shi *et al*., 2015) might mediate the suppression of IFN-β. To test this, we examined poly(dA:dT)- and *F. novicida*-induced IFN-β secretion in wild-type and GSDMD$^{-/-}$ immortalized BMDMs (iBMDMs). We found that, while IL-1β secretion and cell death were reduced, IFN-β production was markedly higher in GSDMD$^{-/-}$ cells, phenocopying AIM2$^{-/-}$ cells (Fig. 2B-D). The augmented production of IFN-β in response to cytosolic DNA was also observed in primary BMDMs from GSDMD$^{-/-}$ mice (Fig. S1B). Furthermore, the kinetic analysis showed sustained hyper-production of IFN-β by *F. novicida*- infected GSDMD$^{-/-}$ BMDMs over a period of time (Fig. 2E). In this time course analysis, GSDMD$^{-/-}$ BMDMs displayed, as expected, reduced LDH release upon *F. novicida* infection. However, there was no difference in the intracellular ATP levels of *F. novicida*-infected wild-type and GSDMD$^{-/-}$ BMDMs (Fig. 2F). In other words, an increase in cytosolic DNA-induced IFN- β production was evident in GSDMD$^{-/-}$ BMDMs without a concomitant increase in intracellular ATP levels. *E. coli* induces IFN-β via TLR4 (Kailasan Vanaja *et al*., 2014; Rathinam *et al*., 2012) and elicits GSDMD activation and cell death via caspase-11 (Fig. 2G) (Kayagaki *et al*., 2015). *E. coli* triggered comparable levels of IFN-β production in wild-type, GSDMD$^{-/-}$ and caspase-11$^{-/-}$ macrophages, indicating that the TLR4-driven IFN-β production is not sensitive to GSDMD-mediated inhibition (Fig. 2G). Sendai virus-induced IFN-β was also comparable between wild-type and GSDMD$^{-/-}$ cells (Fig. 2H). Like IFN-β, cGAS- dependent production of IL-6 was also higher in *F. novicida*-infected GSDMD$^{-/-}$ macrophages (Fig. 2I-K). IFN-β production per cell was measured by intracellular staining followed by flow cytometry for viperin, as a surrogate for IFN-β. This revealed that viperin expression on a per-cell basis as indicated by the mean fluorescence intensity was higher in *F. novicida*- or poly(dA:dT)-,

but not IFN-β-, stimulated GSDMD-deficient cells compared to wild-type cells (Fig. S1C). Unlike GSDMD$^{-/-}$ BMDMs, Nlrp3$^{-/-}$ BMDMs produced IFN-β at a level comparable to wild-type BMDMs upon *F. novicida* infection (Fig. S1D). These results suggest that the AIM2 inflammasome down-regulates type I IFN responses via GSDMD. To test the role of GSDMD in type I IFN response to *F. novicida* infection in vivo, wild-type and GSDMD$^{-/-}$ mice were infected with *F. novicida*, and plasma IFN-β was measured at 24 h p.i. Similar to our observations in vitro in BMDMs, GSDMD-deficient mice had significantly elevated levels of IFN-β in plasma relative to wild-type mice (Fig. 2L). However, the bacterial loads in the spleens and livers of wild-type and GSDMD$^{-/-}$ mice were similar suggesting that the increased IFN-β in GSDMD$^{-/-}$ mice was not due to higher bacterial burden (Fig. 2M). Wild-type and GSDMD$^{-/-}$ mice were infected with *F. novicida* and monitored for survival to address the role of GSDMD in host defense. Notably, GSDMD deficiency compromised the survival of the host as GSDMD-deficient mice succumbed to *F. novicida* infection earlier than WT mice (Fig. 2N). Next, we sought to understand if the elevated IFN-β levels in inflammasome-deficient mice impact host resistance to *F. novicida*. To this end, type I IFN signaling in *F. novicida*-infected AIM2$^{-/-}$ mice was partially blocked with the administration of very low dose of anti-IFNAR antibody (250 mg/mouse) just once (12 h p.i.), and the survival of mice was monitored. Strikingly, anti-IFNAR antibody-treated AIM2$^{-/-}$ mice survived significantly longer than AIM2$^{-/-}$ mice treated with an isotype control antibody (Fig. 2O). In fact, the survival of AIM2$^{-/-}$ mice was rescued to wild-type levels by the anti-IFNAR antibody. This data suggest that the elevated IFN-β in the absence of AIM2 and GSDMD increases the susceptibility of the host to *F. novicida* infection. Consistent with our result with anti-

IFNAR antibody, a latest report showed that the genetic deletion of IFNAR1 in AIM2-deficient mice protected AIM2$^{-/-}$ mice from *F. novicida* infection (Zhu *et al*., 2018). Overall, GSDMD activated by the AIM2 inflammasome reins in the host-detrimental type I IFN expression, promoting anti-bacterial defense.

C. GSDMD targets cGAS to suppress cytosolic DNA-induced IFN-β production.

Upon binding DNA, cGAS catalyzes the synthesis of a second messenger molecule, cGAMP, from ATP and GTP. cGAMP binds to its receptor, STING, and the dimerized STING triggers the activation and self-phosphorylation of TBK1, which in turn phosphorylates IRF3 to initiate IFN-β transcription (Sun *et al*., 2013). To define which step of this pathway is affected by GSDMD, we examined the above-described events in cGAS signaling in wild-type and GSDMD$^{-/-}$ macrophages. *F. novicida* and poly(dA:dT), but not LPS and Sendai virus, induced phosphorylation of TBK1 and IRF3 was substantially higher in GSDMD$^{-/-}$ (Fig. 3A) and AIM2$^{-/-}$ (Fig. 3B) macrophages compared to wild-type cells. These results indicate that the upstream cGAS or STING activation itself is likely to be affected by GSDMD. To explore this, cGAS binding of DNA was assessed by immunoprecipitation of cGAS from *F. novicida*- infected BMDMs followed by PCR analysis of bacterial DNA bound to cGAS. This approach revealed that cGAS in GSDMD$^{-/-}$ BMDMs bound to significantly higher quantity of *F. novicida* DNA than cGAS in wild-type BMDMs suggesting that GSDMD affects cGAS binding of DNA (Fig. 3C-D). Detection of STING dimerization using non-reducing PAGE showed

elevated levels of STING dimers in *F. novicida*- and poly(dA:dT)-, but not cGAMP-stimulated gasdermin-D$^{-/-}$ cells (Fig. 3K), which is in concordance with the higher cGAS activation in the absence of GSDMD. Taken together, these data suggest that GSDMD targets cGAS to suppress cytosolic DNA-induced IFN-β production.

D. GSDMD suppresses cGAS-dependent type I IFN response by triggering potassium (K^+) efflux.

We next sought to define the mechanism involved in the cGAS-suppressive function of GSDMD. Whereas the formation of plasma membrane pores and the cessation of metabolic activity during pyroptosis are not sensitive to glycine, the swelling and terminal rupture of cells is delayed by glycine (Conos *et al*., 2017; Evavold *et al*., 2018; Russo *et al*., 2016). In agreement with the previous reports (Conos *et al*., 2017; Evavold *et al*., 2018; Fink *et al*., 2008; Moltke *et al*., 2012; Rühl and Broz, 2015), glycine greatly reduced *F. novicida*-induced pyroptotic lysis as assessed via LDH release (Fig. 4A) or Cell-Tox Flo assay (Fig. 4B). More relevantly, glycine-treated cells, which were resistant to GSDMD-induced lysis, did not produce excessive amounts of IFN-β in response to *F. novicida* (Fig. 4C). The AIM2 inflammasome catalyzes the maturation of IL-1β and IL-18 via caspase-1 and mediates their release in a GSDMD-dependent manner. Therefore, it is possible that active IL-1β and/or IL-18 can act in an autocrine or paracrine fashion to control the type I IFN responses as shown in the case of M. tuberculosis infection (Mayer-Barber *et al*., 2014). To test this idea, we compared *F. novicida*-induced IFN-β

production in IL-1R- and IL-18R-deficient BMDMs with that of wild-type BMDMs. In contrast to the phenotype in AIM2- and GSDMD-deficient cells, IFN- β response in IL-1R- and IL-18R-deficient BMDMs was comparable to that of wild-type BMDMs (Fig. 4D). Furthermore, to address if there is any redundancy between IL-1β and IL-18 in regulating IFN-β, IL-1β signaling in IL-18r$^{-/-}$ BMDMs was blocked with IL-1R antagonist, and IFN- response to cytosolic DNA was tested. As shown in Fig. 4E, the inhibition of IL-1R signaling with IL-1R antagonist did not affect *F. novicida*-induced IFN-β secretion in IL-18r$^{-/-}$ and WT BMDMs, thus ruling out a role for IL-1β and IL-18 in GSDMD control of IFN-β. The N terminal fragment of GSDMD binds to plasma membrane phospholipids forming pores with an inner diameter of 10 – 15 nm (Aglietti *et al*., 2016; Ding *et al*., 2016; Liu *et al*., 2016; Sborgi *et al*., 2016). These pores permit ionic fluxes across the plasma membrane dissipating intracellular ionic gradients. It is well documented that the formation of GSDMD- pores triggering ionic fluxes is an early event in the cell lytic cascade and is succeeded by water influx, rise in osmotic pressure, cell swelling, the extensive loss of membrane integrity, and eventual lysis (Bergsbaken *et al*., 2009; Evavold *et al*., 2018; Fink and Cookson, 2005). Thus, GSDMD-mediated ion fluxes and the pyroptotic cell death are kinetically separable events (Evavold *et al*., 2018; Katsnelson *et al*., 2015; Moltke *et al*., 2012; Russo *et al*., 2016). Recent reports show that ionic perturbations induced by pore forming proteins govern cellular functions. For instance, ionic fluxes driven by mixed lineage kinase-like (MLKL), the pore forming effector of the necroptotic pathway, has been shown to facilitate plasma membrane repair as well as activate NLRP3 inflammasome prior to cell death (Conos *et al*., 2017; Gong *et al*., 2017; Gutierrez *et al*., 2017). Taking all this into consideration, we reasoned

that GSDMD- mediated ionic fluxes—particularly the efflux of potassium (K^+), which is the most abundant ion in the intracellular milieu with a steep gradient across the plasma membrane—may play a role in the negative regulation of cGAS-dependent type I IFN responses. First, we assessed if inflammasome-mediated GSDMD activation during *F. novicida* infection triggers potassium efflux by utilizing a highly specific potassium stain, APG4 (Eil *et al*., 2016; Prindle *et al*., 2015). We observed that the intracellular levels of K^+ dropped significantly following infection with *F. novicida* in wild-type macrophages but not in macrophages lacking AIM2, caspase-1/11, or GSDMD (Fig. 4F-H). The reductions in intracellular levels of K^+ in wild-type cells was not due to cell lysis as these experiments were performed in the presence of glycine, which prevented cell lysis but not K^+ efflux (Fig. S2A). Next to assess if potassium efflux is required for the GSDMD-mediated suppression of IFN responses, K^+ efflux was diminished by increasing the extracellular concentration of K^+ with KCl (Muñoz-Planillo *et al*., 2013) and its effect on IFN-β secretion was tested. Remarkably, the incubation of wild-type macrophages in DMEM or isosmotic minimal medium supplemented with increasing concentrations of KCl to block K^+ efflux increased poly(dA:dT)- induced IFN-β secretion without affecting pyroptosis or cell viability (Fig. 4I and 4J). The blockade of K^+ efflux similarly enhanced IFN-b secretion following *F. novicida* infection without affecting pyroptosis or cell viability (Fig. 4K and 4L). These results clearly indicate that GSDMD attenuates cGAS-induced type I IFN s by inducing K^+ efflux. An isoleucine-to- asparagine mutation at position 105 (I105N) in the N terminus of GSDMD compromises its capacity to efficiently oligomerize, form pores and presumably induce ionic flux (Aglietti *et al*., 2016). This evidence supports a role for GSDMD-driven pores and ionic flux in the inhibition of cGAS

signaling.

E. K^+ efflux is sufficient to inhibit type I IFN response to cytosolic DNA.

If GSDMD activation dampens IFN-β production in wild-type BMDMs via K^+ efflux as we hypothesize, then pharmacologically restoring K^+ efflux in inflammasome- and GSDMD-deficient cells would reinstate this inhibition and reduce cytosolic DNA-induced type I IFN response back to wild-type levels. We tested this idea by utilizing two well-characterized K^+ ionophores, nigericin and valinomycin (Page and Di Cera, 2006). RAW cells were used in these experiments as they lack ASC and therefore, are resistant to inflammasome-mediated pyroptosis following nigericin and valinomycin stimulation (Fig. S3A). Nigericin and valinomycin induced K^+ efflux in RAW macrophages as assessed by APG4 staining (Fig. 5A and 5B). Consistent with its induction of K^+ efflux, nigericin suppressed IFN-β production by RAW cells following *F. novicida* infection and poly(dA:dT) transfection (Fig. 5A and 5C). But nigericin did not inhibit TLR-mediated IFN-β response to LPS and poly(I:C) (Fig. 5C). This result suggest that the suppressive effect of nigericin on *F. novicida*- and poly(dA:dT)-induced IFN-β production is neither due to global shut down of IFN-β expression nor cytotoxicity. Similar to nigericin, valinomycin impaired RAW cell production of IFN-β following *F. novicida* and poly(dA:dT) stimulations (Fig. 5B). Unlike these K^+ ionophores, the calcium ionophore, ionomycin, did not affect *F. novicida*-induced IFN-β secretion (Fig. S3B). Similarly, the calcium chelator, BAPTA- AM, had no effect on IFN-β response to cytosolic DNA (Fig.

S3C). These results, thus, rule out a role for calcium influx in type I IFN inhibition by GSDMD. Nigericin treatment reduced cGAMP levels in *F. novicida*- and poly(dA:dT)-stimulated RAW cells, supporting the notion that GSDMD targets cGAS via K^+ efflux (Fig. 5D). In agreement with the impairment of cGAS activation by K^+ efflux, nigericin reduced TBK1 and IRF3 activation in RAW macrophages in response to poly(dA:dT) but not LPS (Fig. 5E). These results indicate that K^+ efflux targets the cytosolic cGAS-STING-mediated IFN-β response but not TLR-initiated type I IFN responses. Next, we used caspase-1/11$^{-/-}$ macrophages to validate these findings. Compared to *F. novicida*-infected wild-type cells, caspase-1/11$^{-/-}$ BMDMs had higher levels of intracellular K^+ and secreted increased levels of IFN-β (Fig. 5F and 5G). Addition of nigericin or valinomycin to caspase-1/11$^{-/-}$ BMDMs lowered intracellular K^+ content and correspondingly reduced IFN-β production (Fig. 5F and 5G). Importantly, this IFN-β reduction upon nigericin and valinomycin treatments was not due to cell death as the caspase-1/11 deficiency and the use of very low amounts of nigericin and valinomycin circumvented nigericin- and valinomycin-induced cell death (Fig. S3D). It should also be noted that while cytosolic DNA-induced IFN-β secretion by caspase-1/11$^{-/-}$ BMDMs was tremendously diminished by nigericin or valinomycin, LPS- and poly(I:C)-induced IFN-β secretion remained unaffected (Fig. 5H). Similarly, the incubation of caspase-1/11$^{-/-}$ macrophages in K^+ free medium, which is known to trigger K^+ efflux (Rühl and Broz, 2015), diminished their higher IFN-β production, in response to *F. novicida* and poly(dA:dT), to levels comparable to that of wild-type cells (Fig. 5I). On the other hand, poly(I:C)-induced IFN-β production was not affected by the potassium levels of the medium (Fig. 5I). The increased IFN-β secretion by *F. novicida*-infected GSDMD-deficient macrophages was

also reduced to wild-type levels by nigericin and valinomycin without affecting cell death (Fig. 5J, 5K, and S3D). In contrast, IFN-β production by GSDMD- deficient macrophages in response to TLR4 and TLR3 activation was not suppressed by nigericin and valinomycin (Fig. 5L). Furthermore, detailed dose response experiments in WT, GSDMD$^{-/-}$, caspase-1/11$^{-/-}$, and RAW macrophages showed that extremely low concentrations of nigericin (20-50 nM) are able to inhibit *F. novicida*- and poly(dA:dT)-induced IFN-β response without affecting cell viability and metabolic activity as indicated by CellTiter-Glo and PrestoBlue assays (Fig. 5M-O and S4A-C). Minimal concentrations of valinomycin (50-100 nM) also decreased IFN-β response to cytosolic DNA without reducing cell viability and metabolic activity (Fig. S4D). More importantly, K^+ free media-induced reduction in IFN-β production was reversed when KCl was returned to culture medium (Fig. 5P) indicating that the cells remained viable during exposure to K^+ free media. Likewise, nigericin-induced reduction in IFN-β production was reversed when the K^+ ionophore was replaced from culture medium (Fig. S4E). Altogether, the striking effects of K^+ efflux blockade and K^+ efflux induction by pharmacological (K^+ ionophores) and non-pharmacological (K^+ free medium) means on IFN-β production in multiple cell types provide substantial evidence that K^+ efflux is necessary and sufficient to inhibit cytosolic DNA-induced type I IFN response. The data reinforces that K^+ ion is critical for cGAS catalytic activity and the depletion of its intracellular levels by GSDMD pores impairs cGAS function independent of cell death.

Chapter IV

Discussion

Gasdermin-D suppresses cytosolic DNA-induced type-I IFN production by inducing K^+ efflux.

The c-GAS DNA sensor is an important pathway in the host cell for mounting an immune response to cytosolic pathogens. cGAS senses pathogen DNA and also host cell DNA that leaks into the cytosol during some pathological condition. It signals through the adapter STING, kinase TBK-1 and transcription factor IRF3 that induces the production of type-I IFN (Sun *et al*., 2013). Although type–I IFN has a beneficial role in viral and some bacterial infections, its excessive signaling is detrimental in some intracellular bacterial infections and can result in pathology in autoimmune and inflammatory diseases.

The release DNA in the cytosol of macrophages is recognized by sensors cGAS and AIM2 in macrophages. In contrast to cGAS, AIM2 sensing of DNA leads to the assembly and the activation of the inflammasome complex (Hornung and Latz, 2010). Our findings show that similar to prior reports in literature; cytosolic DNA induced activation of the inflammasome complex suppressed the production of type-I IFN production both *in-vitro* and *in-vivo* (Fig. 1; Corrales *et al*., 2016; Fernandes-Alnemri *et al*., 2010; Gray *et al*., 2016; Hornung *et al*., 2009; Jones *et al*., 2010; Rathinam *et al*., 2010; Wang *et al*., 2010). Inflammasome activation in turn leads to the cleavage and activation of GSDMD. We further showed that similar to mice deficient in inflammasome components ($AIM2^{-/-}$ and caspase-$1/11^{-/-}$) $GSDMD^{-/-}$ also show increased type-I IFN production. GSDMD deficient animals are more susceptible to *F. novicida* infection due

to the detrimental effects of heightened type-I IFN produced in these animals (Fig.2). GSDMD is cleaved into its N- and C-terminus domains. N-terminus of GSDMD oligomerizes and forms pores in the plasma membrane. These non-selective pores formed by GSDMD leads to the exchange of fluids and ions. The exchange of ions through a non-selective pore depends on the ion gradient across the cell membrane. K^+ has a high concentration in the cytosol compared to the extracellular fluid. Therefore, formation of GSDMD pores leads to K^+ efflux (Aglietti *et al*., 2016; Ding *et al*., 2016; Kovacs and Miao, 2017; Liu *et al*., 2016; Sborgi *et al*., 2016). This study reports that the depletion of intracellular K^+ from the cell inhibits cGAS detection of DNA. Thereby, restraining cytosolic DNA-induced type-I IFN production (Fig 3, 4,5).

Many recent studies have attempted to separate the established role of GSDMD in cell death from new roles in a variety of cellular functions. Inflammasome activation results in the secretion of IL-1β and IL-18. These two IL-1 family members, similar to rest of the cytokines of the group lack the signal peptide for conventional protein secretion through the ER and golgi apparatus. These cytokines are released from the cell using an alternative secretory pathway.

Recent reports have shown that this release is dependent on GSDMD. Evavold *et al*., using stimuli that do not cause pyroptosis but results in the cleavage of GSDMD have demonstrated that IL-1β is released from non-pyroptotic cells in a GSDMD dependent manner (Evavold *et al*., 2018). GSDMD has also been reported to be essential for the formation of NETs from neutrophils in extracellular bacterial infections independent of pyroptosis (Chen *et al*., 2018; Sollberger *et al*., 2018). Further, consolidating the

evidence that GSDMD is essential for cellular functions not restricted to pyroptosis.

This study provides multiple lines of evidence showing that regulation of type-I IFN production by GSDMD can be separated from its role in pyroptosis

1. Inhibiting K^+ efflux by neutralizing the extracellular ionic gradient by adding KCl to the extracellular media increases the IFN level without any change in cell death.
2. Inducing K^+ efflux in inflammasome and GSDMD deficient cells using chemical agents such as nigericin that acts as K^+ ionophore in inflammasome deficient cells and at very low doses does not affect the viability of the cell.
3. K^+-free media and K^+ ionophore mediated inhibition was reversible.
4. In a cell free system, K^+ concentration can regulate the amount of cGAMP production by cGAS.

The kinetics of these events dictate whether GSDMD can impact other functions in the cell.

The formation of GSDMD pores in the plasma membrane disrupts the normal concentration of ions across the plasma membrane. K^+ has a high concentration in the cytoplasm and a low concentration in the extracellular milieu therefore disruption of the plasma membrane barrier by formation of GSDMD pores leads to the efflux of K^+ ions. Sodium (Na) has the reverse gradient. There is an influx of Na^+ in the cell that is accompanied by water resulting in cell swelling (Kovacs and Miao, 2017). The GSDMD pore is 10-15 nm in diameter and therefore K^+ that are 0.2 nm or mature forms of IL-1β

or IL-18 that are 4.5 and 5 nm in diameter respectively can pass through the GSDMD pores but cell organelles that are larger than 15 nm cannot leak out, thereby maintaining cell integrity (Ding *et al*., 2016; Liu *et al*., 2016). The concentration of cleaved GSDMD and thereby, the number of pores formed in the cell membrane is a determinant of whether the cell will undergo pyroptosis. Therefore, repair mechanisms can patch-up the plasma membrane if GSDMD pores are below a certain threshold.

Our results as previously described reports that K^+ efflux from the cell can regulate DNA-induced type-I IFN production; thereby demonstrating the key role of K^+ in GSDMD mediated suppression. The evidence in literature shows that K^+ plays a key role in enzyme catalysis. K^+ is abundant inside the cell and many cellular processes use it as a source of chemical potential to drive enzymatic catalysis (Gohara and Di Cera, 2016). The data in this study, using a cGAS enzymatic assay demonstrates that K^+ plays a role in cGAS-DNA interaction.

This correlates with recent studies. Wang *et al*., show that Manganese (Mn) increases the sensitivity of cGAS-DNA interactions as well as its enzymatic activity in DNA virus infections (Wang *et al*., 2018). Another example of ion concentration influencing cGAS activity comes from the evidence that Zinc (Zn) enhances the catalytic activity of cGAS both in-vitro and in cell systems (Du and Chen, 2018).

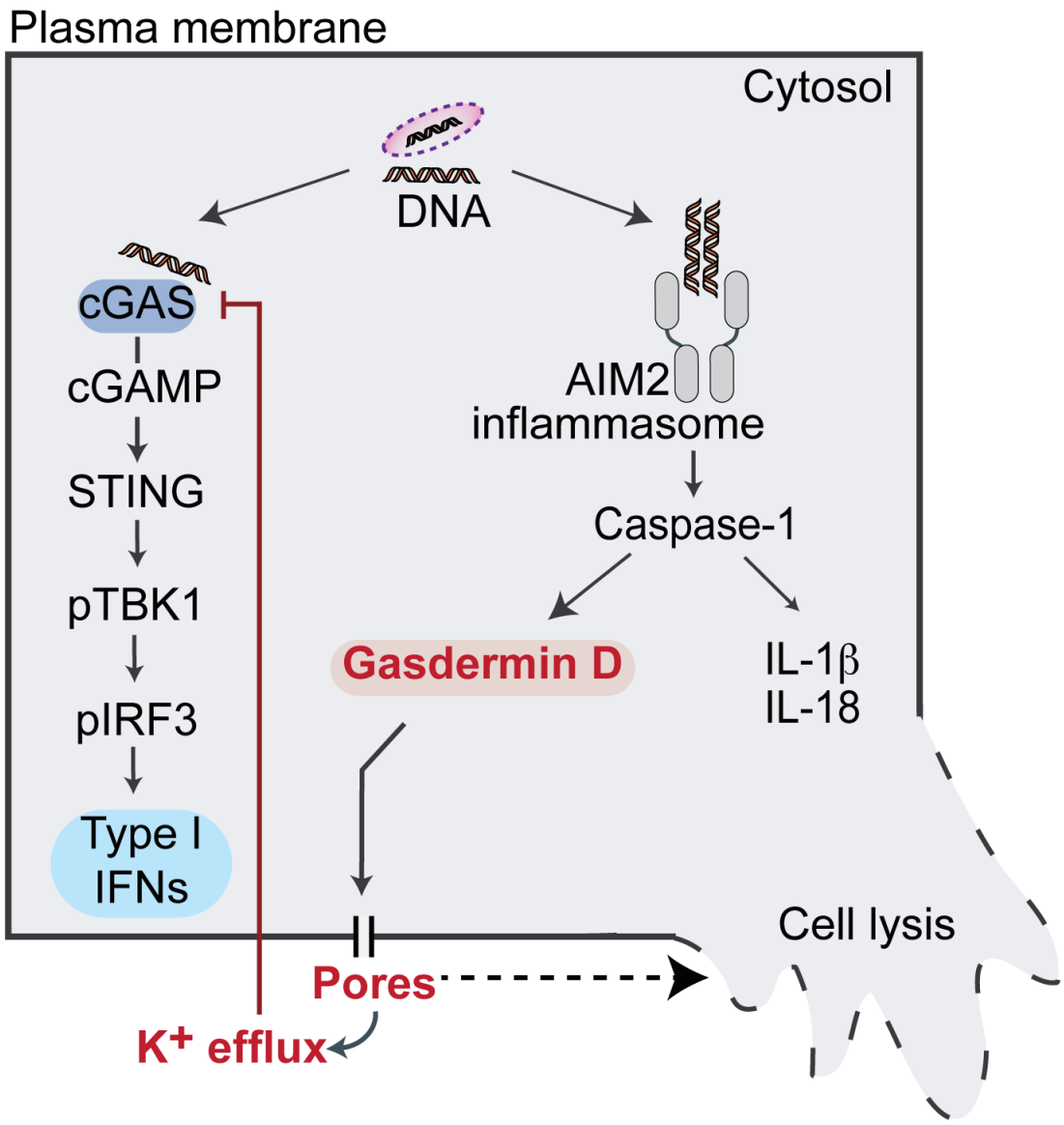

Figure 1: Summary: Gasdermin-D suppresses cytosolic DNA-induced type-I IFN production by inducing K^+ efflux.

DNA in the cytoplasm activates cGAS-STING mediated IFN-β production and AIM2 inflammasome induced GSDMD activation. GSDMD forms pores in the plasma membrane resulting in K^+ efflux. The reduction in intracellular K^+ concentration abrogates cGAS-DNA interactions, thereby suppressing the production of type-I IFN (Banerjee *et al*., 2018).

Significance

Pathological conditions such as cancer can result in damage to the nuclear compartment. This can result in the presentation of the nuclear material to cytoplasmic host sensors. Nuclear self-DNA can thus be recognized by cytoplasmic DNA sensors cGAS and AIM2 (Di Micco *et al*., 2016). cGAS recognition of self DNA from dying tumor cells results in the production of type-I IFNs (Corrales *et al*., 2016). Additionally, cGAS mediated IFN production is essential for priming of CD8 T cells against tumor antigens (Deng *et al*., 2014). Moreover, intra-tumoral delivery of cGAMP leads to increased tumor regression and prolonged survival of tumor-bearing mice (Corrales *et al*., 2015; Demaria *et al*., 2015). cGAMP has also shown to be beneficial in combinatorial therapy with check-point blockade therapy such as antibodies against PD-1 and PD-L1 (Chen *et al*., 2016).

Activation of the inflammasome pathway by self-DNA can lead to the development of autoinflammatory diseases such as polyarthritis like symptoms caused in DNase II deficient mice (Baum *et al*., 2015; Jakobs *et al*., 2015). One of the most prominent auto-inflammatory diseases associated with dysrerulated cGAS induced type-I IFN production is Acardi-Goutiers Syndrome. These patients typically have genetic defects in the exonuclease TREX-1that degrades single-stranded DNA or RNaseH2 that cuts RNA in RNA-DNA hybrids (Gao *et al*., 2015; Gray *et al*., 2015; McKenzie *et al*., 2016). Another auto-inflammatory disease associated with gain-of function mutations in STING is called STING-associated vasculopathy (SAVI) (Liu *et al*., 2014). Patients with this

syndrome typically present with cutaneous inflammation, ulcers and necrotizing lesions and widespread pulmonary damage (Reviewed in: Chen *et al*., 2016).

Therefore, the discovery of a novel regulatory mechanism for cGAS/STING-induced type-I IFN may have profound therapeutic implications in anti-tumor immunity and auto-inflammatory and autoimmune diseases.

Chapter V

Figures

Results of the presented work have been published in Banerjee *et al.*, 2018.

Fig. 1

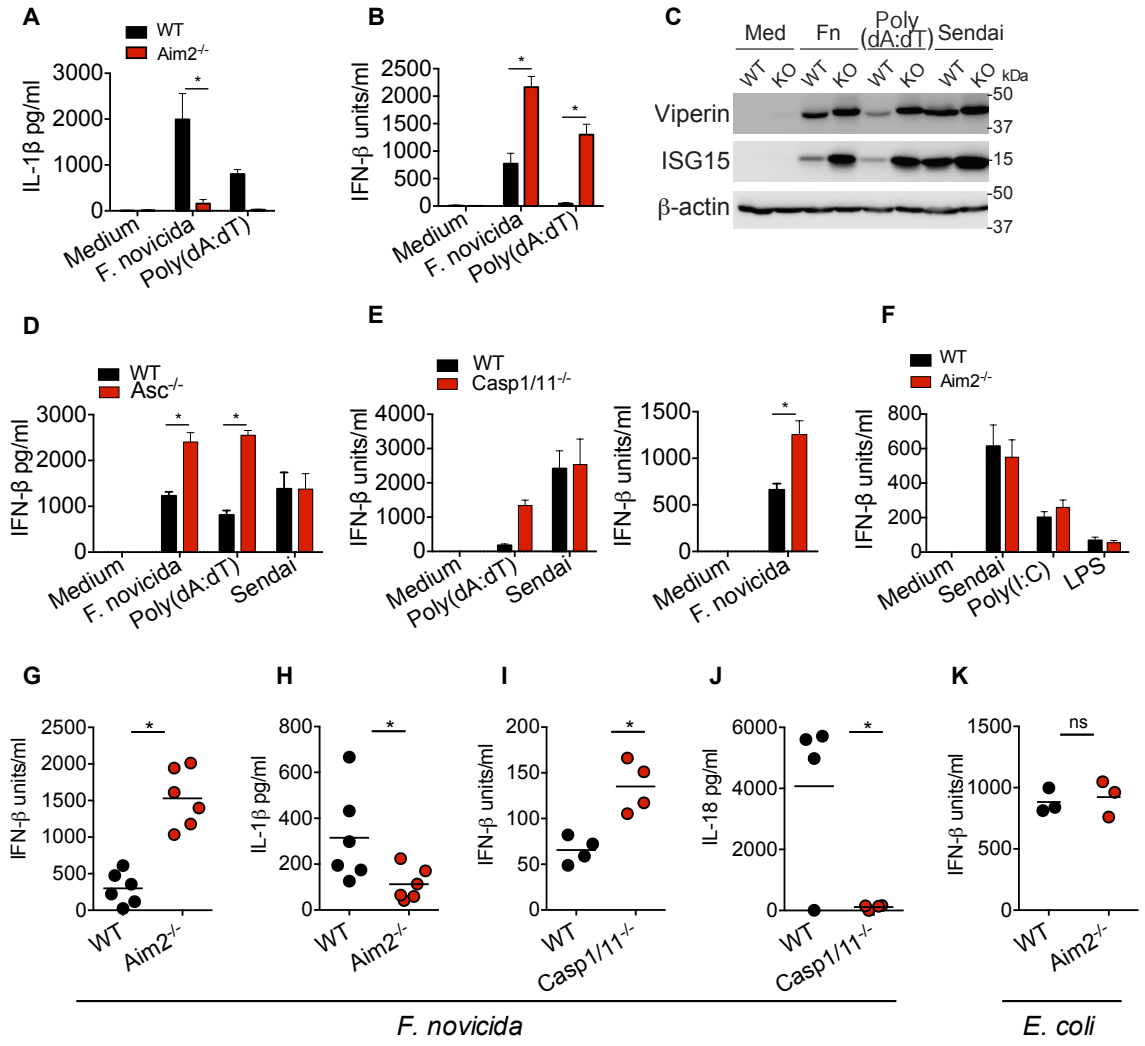

Figure 1.

AIM2 inflammasome activation suppresses cytosolic DNA-induced type I IFN production.

(A and B) IL-1 β (A) and IFN-β (B) levels in the supernatants of Pam3CSK4-primed wild-type (WT) and AIM2$^{-/-}$ BMDMs stimulated with *F. novicida* (MOI=50) or poly(dA:dT) for 6 h. (C) Immunoblots of viperin, ISG15 and b-actin in the lysates of WT and AIM2$^{-/-}$ (KO) iBMDMs stimulated with *F. novicida* (MOI=100), poly(dA:dT), or Sendai virus for 8 h. (D to F) IFN- β levels in the supernatants of BMDMs from WT, Asc$^{-/-}$ (D), Caspase-1/11$^{-/-}$ (E), and AIM2$^{-/-}$ (F) mice stimulated with indicated treatments for 6 h. (G-J) Cytokine levels in the plasma of WT or indicated KO mice infected s.c. with 5 Å~ 105 CFU of *F. novicida*. Cytokine levels were assessed 24 h post-infection (p.i). (K) Plasma IFN-b levels in WT and AIM2$^{-/-}$ mice 6 h after intraperitoneal infection with 1 Å~ 109 CFU of E. coli BL21. Data are from one experiment representative of three. In the bar graphs, data are presented as mean±SEM, and each dot represents a technical replicate. For G-K, each circle represents a mouse and the horizontal lines represent mean. IFN- β levels are presented as units/ml or pg/ml depending upon the recombinant IFN-β standard used in the ELISA. *, P <0.05; ns, not significant; two-way ANOVA followed by the Sidak's post-test (A, B, D, and E) or unpaired two- tailed t test (G-K).

Fig. 2

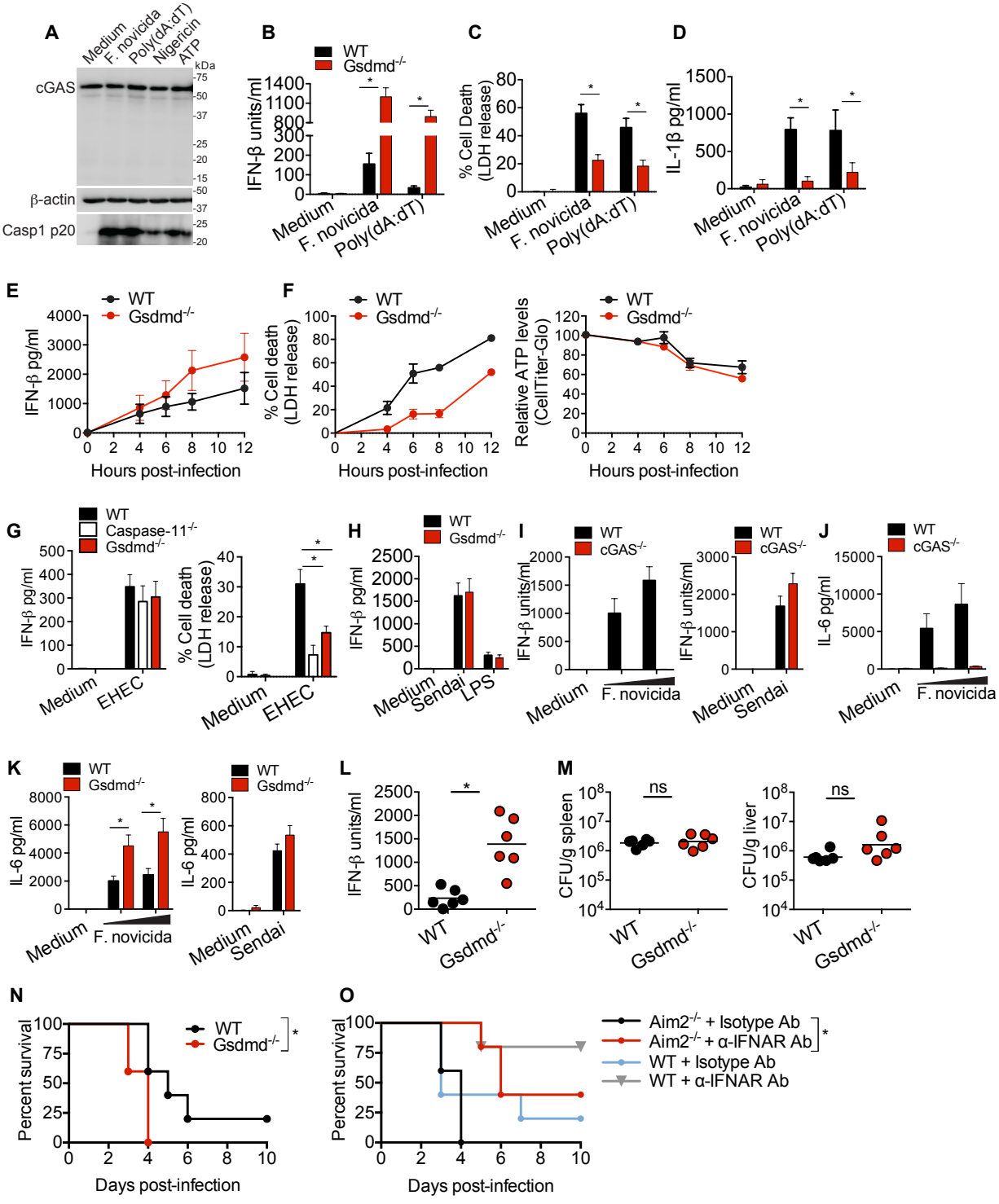
A
Medium
F. novicida
Poly(dA:dT)
Nigericin
ATP
kDa
cGAS
β-actin
Casp1 p20
B
WT
Gsdmd-/-
IFN-β units/ml
C
% Cell Death (LDH release)
D
IL-1β pg/ml
E
IFN-β pg/ml
Hours post-infection
F
% Cell death (LDH release)
Relative ATP levels (CellTiter-Glo)
G
Caspase-11-/-
EHEC
H
Sendai
LPS
I
cGAS-/-
F. novicida
J
IL-6 pg/ml
K
L
M
CFU/g spleen
CFU/g liver
ns
N
Percent survival
Days post-infection
O
Aim2-/- + Isotype Ab
Aim2-/- + α-IFNAR Ab
WT + Isotype Ab
WT + α-IFNAR Ab

Figure 2.

GSDMD is required for inflammasome-mediated suppression of type I IFN production.

(A) Immunoblotting for cGAS and b-actin in the lysates and the cleaved caspase-1 (p20) in the methanol chloroform-precipitated supernatants of Pam3CSK4-primed WT BMDMs stimulated with *F. novicida*, poly(dA:dT), nigericin, or ATP. (B-D) IFN-β secretion (B), cell death (C), and IL-1 β secretion (D) by Pam3CSK4-primed WT and GSDMD$^{-/-}$ iBMDMs stimulated with *F. novicida* or poly(dA:dT) for 6 h. (E-F) IFN-β secretion (E), LDH release, and intracellular ATP levels (F) in WT and GSDMD$^{-/-}$ primary BMDMs infected with *F. novicida* (MOI=100) at 4, 6, 8 and 12 h p.i. (G) IFN-β secretion and cell death in WT, caspase-11$^{-/-}$ and GSDMD$^{-/-}$ primary BMDMs infected with EHEC (MOI=50) at 16 h p.i.

(H) IFN-β levels in the supernatants of WT and GSDMD$^{-/-}$ BMDMs stimulated with Sendai virus or LPS for 6 h. (I-K) IFN-β (I) or IL-6 (J and K) levels in the supernatants of BMDMs of indicated genotypes infected with *F. novicida* (MOI of 12.5, 25 and 50) or Sendai virus for 6 h. (L and M) IFN-β levels in the plasma (L) and the bacterial load in the spleen and liver (M) of WT and GSDMD$^{-/-}$ mice infected s.c. with 1.5 Å~ 105 CFU of *F. novicida* at 24 h p.i. Each circle represents a mouse and the horizontal lines represent mean. (N) Survival of WT and GSDMD$^{-/-}$ mice (n=5) infected s.c. with 2.5 Å~ 102 CFU of *F. novicida*. (O) Survival of WT and AIM2$^{-/-}$ mice (n=5) infected s.c. with 2.5 Å~ 102 CFU of *F. novicida* and injected i.p. with 250 mg of an isotype control or anti-IFNAR antibody 12 h p.i. Data are from one experiment representative of three (A-M) or

two (N and O) experiments. In the bar graphs, data are presented as mean±SEM, and each dot represents a technical replicate. For L-M, each circle represents a mouse and the horizontal lines represent mean. IFN-β levels are presented as units/ml or pg/ml depending upon the recombinant IFN-β standard used in the ELISA. *, $P < 0.05$; ns, not significant; two-way ANOVA followed by the Sidak's post-test (B, C, D, and G), unpaired two-tailed t test (L and M), or Mantel-Cox test (N and O). See also Figure S1.

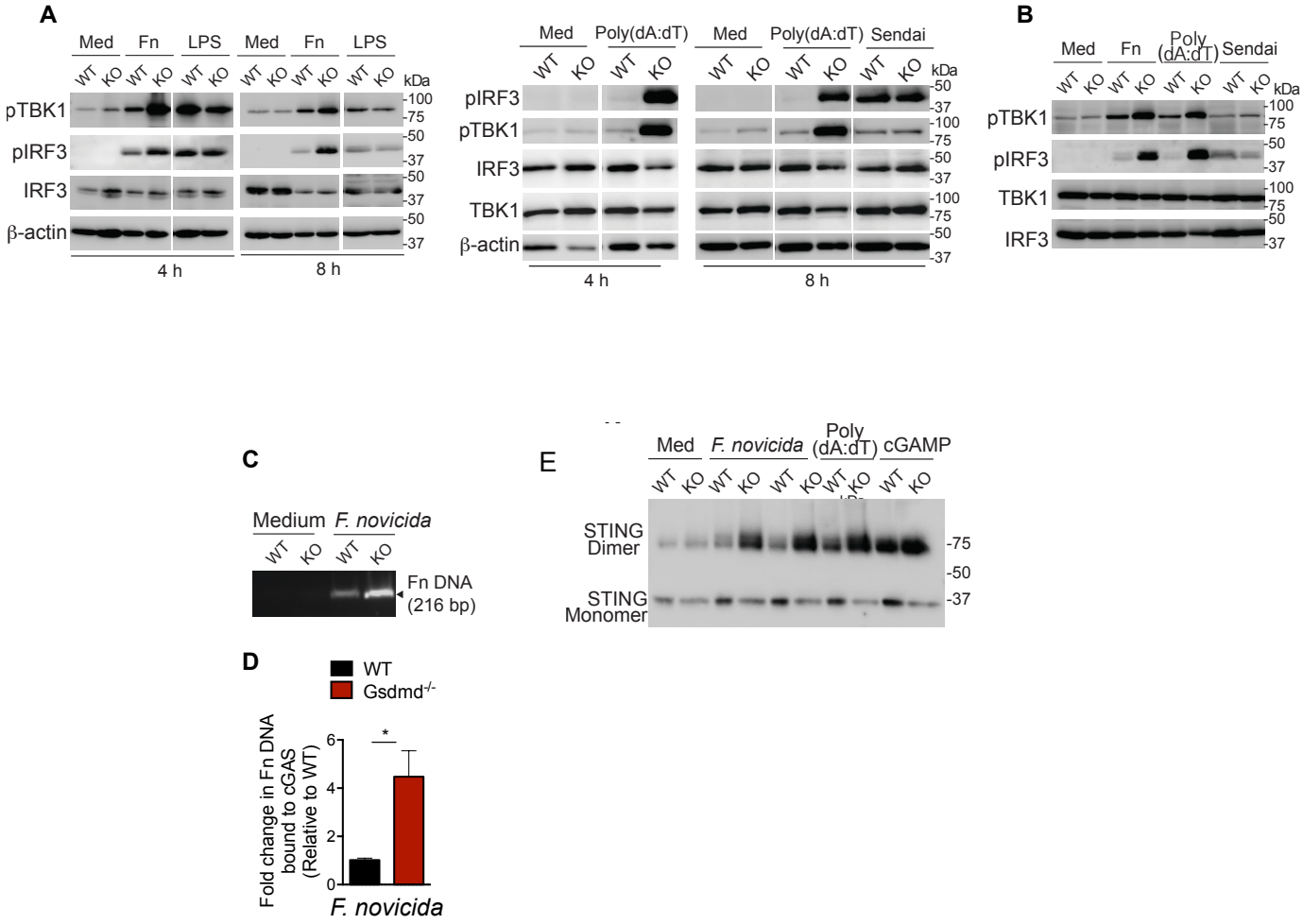
A
Med
Fn
LPS
WT
KO
kDa
pTBK1
pIRF3
IRF3
β-actin
4 h
8 h
Poly(dA:dT)
Sendai
TBK1
B
C
Medium
F. novicida
Fn DNA
(216 bp)
D
WT
Gsdmd-/-
Fold change in Fn DNA bound to cGAS (Relative to WT)
E
cGAMP
STING Dimer
STING Monomer

Figure 3.

GSDMD suppresses cytosolic DNA-induced IFN-β by targeting cGAS.

(A) Immunoblots of pIRF3, pTBK1, IRF3, and β-actin in the lysates of WT and GSDMD$^{-/-}$ BMDMs stimulated with indicated treatments for indicated times. Med, medium; Fn, *F. novicida*. (B) Immunoblots of pIRF3, pTBK1, IRF3, TBK1, and β-actin in the lysates of WT and AIM2$^{-/-}$ BMDMs stimulated with indicated treatments for 8 h. SeV, Sendai virus. (C-D) PCR analysis of *F. novicida* DNA recovered from cGAS immunoprecipitates from WT and GSDMD$^{-/-}$ BMDMs stimulated with *F. novicida* for 6 h. Agarose gel image of PCR products (C). Fold increase in cGAS-associated *F. novicida* DNA in GSDMD$^{-/-}$ BMDMs over that of wild-type BMDMs as revealed by quantitative PCR (D). Fn, *F. novicida*. (E) STING monomers and dimers in the lysates of WT and GSDMD$^{-/-}$ BMDMs stimulated with *F. novicida* (MOIs of 50 and 100), poly(dA:dT), or cGAMP for 6 h as assessed by nonreducing PAGE and immunoblotting. Med, medium. Data presented as mean±SEM are from one experiment representative of three. Each dot represents a technical (D) replicate. *, $P < 0.05$; ns, not significant; unpaired two-tailed t test (D).

Fig. 4

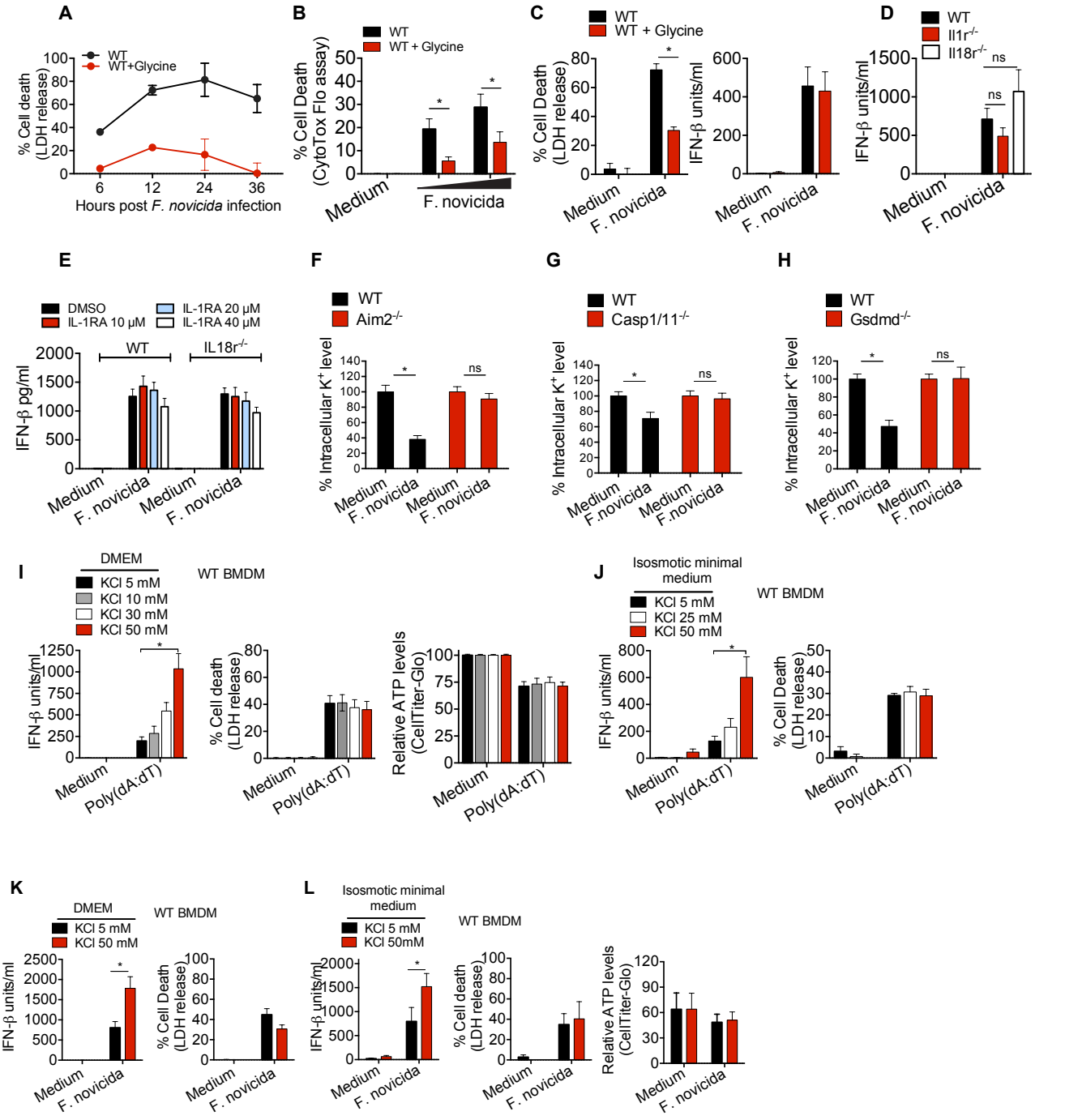
A
% Cell death (LDH release)
WT
WT+Glycine
Hours post F. novicida infection
B
% Cell Death (CytoTox Flo assay)
WT
WT + Glycine
Medium
F. novicida
C
% Cell Death (LDH release)
IFN-β units/ml
WT
WT + Glycine
D
IFN-β units/ml
WT
Il1r-/-
Il18r-/-
ns
E
IFN-β pg/ml
DMSO
IL-1RA 10 μM
IL-1RA 20 μM
IL-1RA 40 μM
WT
IL18r-/-
F
% Intracellular K+ level
WT
Aim2-/-
G
% Intracellular K+ level
WT
Casp1/11-/-
H
% Intracellular K+ level
WT
Gsdmd-/-
I
DMEM
KCl 5 mM
KCl 10 mM
KCl 30 mM
KCl 50 mM
WT BMDM
IFN-β units/ml
% Cell death (LDH release)
Relative ATP levels (CellTiter-Glo)
Poly(dA:dT)
J
Isosmotic minimal medium
KCl 5 mM
KCl 25 mM
KCl 50 mM
WT BMDM
IFN-β units/ml
% Cell Death (LDH release)
K
DMEM
KCl 5 mM
KCl 50 mM
WT BMDM
IFN-β units/ml
% Cell Death (LDH release)
L
Isosmotic minimal medium
KCl 5 mM
KCl 50mM
WT BMDM
IFN-β units/ml
% Cell death (LDH release)
Relative ATP levels (CellTiter-Glo)

Figure 4.

GSDMD suppresses type I IFN production by inducing K^+ efflux.

(A) Cell death in WT BMDMs infected with *F. novicida* for 6, 12, 24 and 36 h in the presence or absence of glycine as assessed by LDH release. (B) Cell death in WT BMDMs infected with *F. novicida* for 6 h in the presence or absence of glycine as assessed by CytoTox Flo assay. (C) Cell death in and secretion of IFN-β by WT BMDMs infected with *F. novicida* for 6 h in the presence or absence of glycine. (D) IFN-β levels in the supernatants of WT, $IL1r^{-/-}$ or $IL18r^{-/-}$ BMDMs following infection with *F. novicida* for 6 h. (E) IFN-β levels in the supernatants of *F. novicida*-infected WT and $IL18r^{-/-}$ BMDMs treated with DMSO or IL-1R antagonist at the indicated concentrations. (F-H) Intracellular K^+ levels as assessed by APG4 staining in WT, $AIM2^{-/-}$ (F), Caspase-$1/11^{-/-}$ (G), and $GSDMD^{-/-}$ (H) in uninfected and *F. novicida*-infected BMDMs at 6 h p.i. (in the presence of glycine). (I to L) IFN- β secretion, cell death (assessed by LDH release assay), and cell viability (assessed by CellTiter-Glo assay) in WT BMDMs stimulated with poly(dA:dT) or *F. novicida* as indicated for 6 h in DMEM (I and K) or isosmotic minimal medium (J and L) supplemented with indicated amounts of KCl.

Data presented as mean±SEM are from one experiment representative of three. Each dot represents a technical replicate. IFN-β levels are presented as units/ml or pg/ml depending upon the recombinant IFN-β standard used in the ELISA. *, $P < 0.05$; ns, not significant; two-way ANOVA followed by the Sidak's post-test. See also Figure S3.

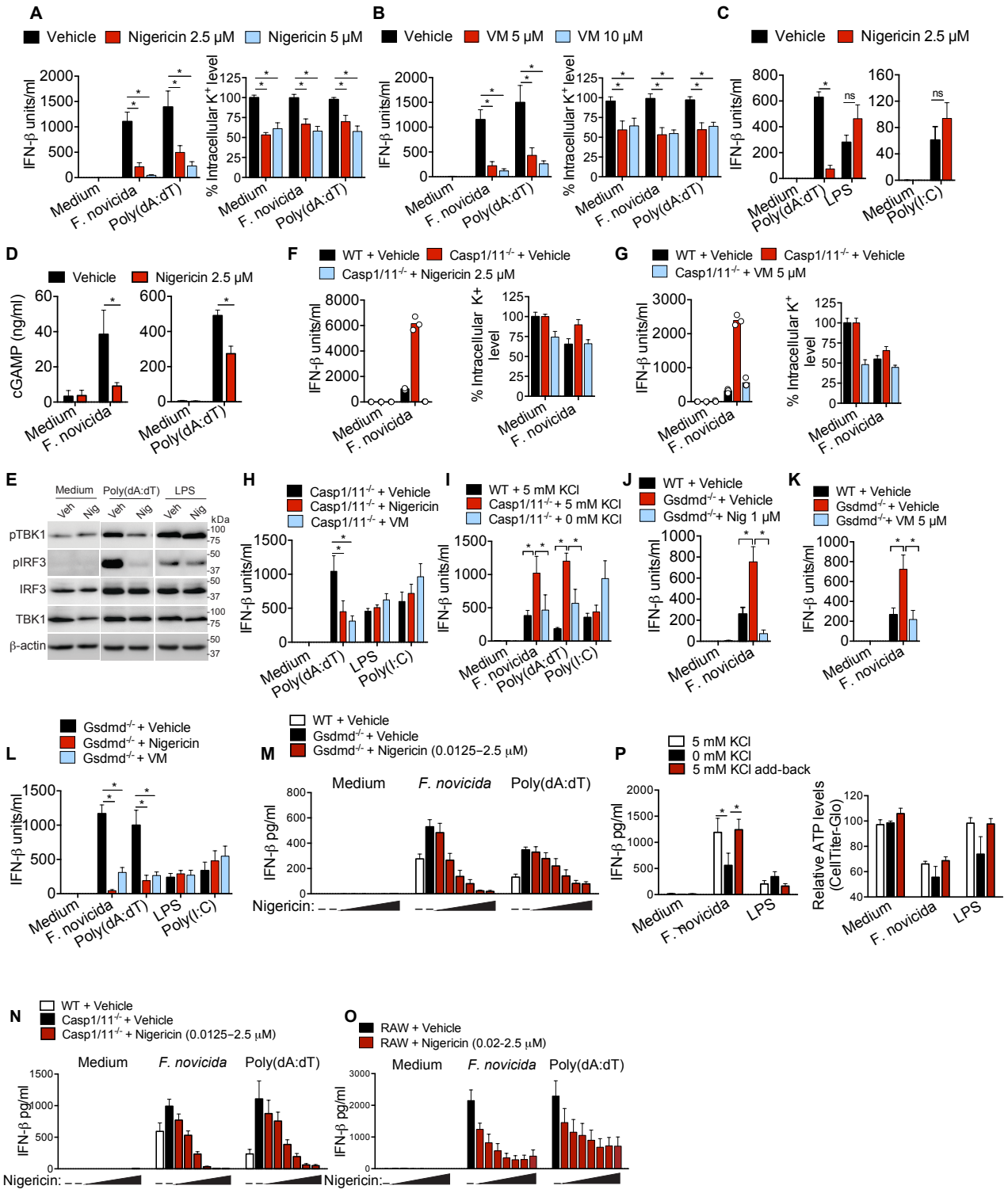
A
Vehicle
Nigericin 2.5 μM
Nigericin 5 μM
IFN-β units/ml
% Intracellular K+ level
Medium
F. novicida
Poly(dA:dT)
B
Vehicle
VM 5 μM
VM 10 μM
C
Vehicle
Nigericin 2.5 μM
LPS
Poly(I:C)
ns
D
cGAMP (ng/ml)
E
Medium
Poly(dA:dT)
LPS
Veh
Nig
kDa
pTBK1
pIRF3
IRF3
TBK1
β-actin
F
WT + Vehicle
Casp1/11-/- + Vehicle
Casp1/11-/- + Nigericin 2.5 μM
G
Casp1/11-/- + VM 5 μM
H
Casp1/11-/- + Nigericin
Casp1/11-/- + VM
I
WT + 5 mM KCl
Casp1/11-/- + 5 mM KCl
Casp1/11-/- + 0 mM KCl
J
WT + Vehicle
Gsdmd-/- + Vehicle
Gsdmd-/- + Nig 1 μM
K
Gsdmd-/- + VM 5 μM
L
Gsdmd-/- + Vehicle
Gsdmd-/- + Nigericin
Gsdmd-/- + VM
M
WT + Vehicle
Gsdmd-/- + Vehicle
Gsdmd-/- + Nigericin (0.0125–2.5 μM)
IFN-β pg/ml
Nigericin:
P
5 mM KCl
0 mM KCl
5 mM KCl add-back
Relative ATP levels (CellTiter-Glo)
N
WT + Vehicle
Casp1/11-/- + Vehicle
Casp1/11-/- + Nigericin (0.0125–2.5 μM)
O
RAW + Vehicle
RAW + Nigericin (0.02-2.5 μM)

Figure 5.

Induction of K^+ efflux in inflammasome-deficient macrophages is sufficient to restore cytosolic DNA-induced type I IFN response to wild-type levels.

(A and B) IFN-β levels in the supernatants of and intracellular K^+ levels (at 6 h post-stimulation) in RAW macrophages stimulated with *F. novicida* (MOI of 50) or poly(dA:dT) and treated at 2 h after stimulations with vehicle (ethanol), 2.5 or 5 mM nigericin (A) or 5 or 10 mM valinomycin (VM; B). (C) IFN-β levels in the supernatants of RAW macrophages stimulated with poly(dA:dT), LPS (1 mg/ml) or poly(I:C) (40 mg/ml) and treated at 2 h after stimulations with 2.5 mM nigericin. (D) cGAMP levels in RAW macrophages 5 h after stimulated with *F. novicida* or poly(dA:dT) and treated at 2 h after stimulations with 2.5 mM nigericin. as measured by LC-MS. (E) Immunoblots of pIRF3, pTBK1, IRF3, TBK1 and b-actin in lysates of RAW macrophages stimulated with poly(dA:dT) or LPS and treated with vehicle (Veh) or 2.5 mM nigericin (Nig). (F and G) IFN-β levels in the supernatants of and intracellular K^+ levels in WT and caspase-1/11-/- BMDMs (measured at 6 h post-infection) infected with *F. novicida* and treated with vehicle (ethanol), 2.5 mM nigericin (F), or 5 mM valinomycin (VM; G) 2 h post-infection. (H) IFN-β levels in the supernatants of caspase-1/11$^{-/-}$ BMDMs (measured at 6 h post-stimulation) stimulated with poly(dA:dT), LPS, or poly(I:C) and treated with vehicle, 2.5 mM nigericin or 5 mM valinomycin (VM). (I) IFN-β levels in the supernatants of *F. novicida*-, poly(dA:dT)-, or poly(I:C)-stimulated WT BMDMs incubated in isosmotic minimal medium containing 5 mM KCl and caspase-1/11$^{-/-}$ BMDMs incubated in isosmotic minimal medium containing 5 or 0 mM KCl. (J and K) IFN-β levels in the

supernatants of WT and GSDMD$^{-/-}$ iBMDMs (measured at 6 h post-infection) infected with *F. novicida* and treated with vehicle, nigericin (J), or valinomycin (VM; K) at the indicated concentrations 2 h post-infection. (L) IFN-β levels in the supernatants of GSDMD$^{-/-}$ iBMDMs (measured at 6 h post-stimulation) stimulated with *F. novicida*, poly(dA:dT), LPS, or poly(I:C) and treated with vehicle, 2.5 mM nigericin, or 5 mM valinomycin (VM).

(M-O) IFN-β levels in the supernatants of indicated macrophages (at 6 h post-stimulation) stimulated with *F. novicida* (MOI of 50) or poly(dA:dT) and treated at 1.5 – 2 h after stimulations with vehicle (ethanol) or increasing concentrations of nigericin (0.0125–2.5 mM). (P) IFN-β levels in the supernatants of and intracellular ATP levels in GSDMD$^{-/-}$ BMDMs (at 6 h post-stimulation) stimulated with *F. novicida* or LPS. After 1 h of stimulation cells were incubated in isosmotic minimal medium containing 5 mM or no KCl and 1 h later, KCl was added to cells incubated in isosmotic minimal medium without KCl to restore K^+ concentration in the medium to 5 mM. Data presented as mean±SEM are from one experiment representative of three. Each dot represents a technical replicate. IFN-β levels are presented as units/ml or pg/ml depending upon the recombinant IFN-β standard used in the ELISA. *, P <0.05; ns, not significant; two-way ANOVA followed by the Sidak's post-test. See also Figures S3 and S4.

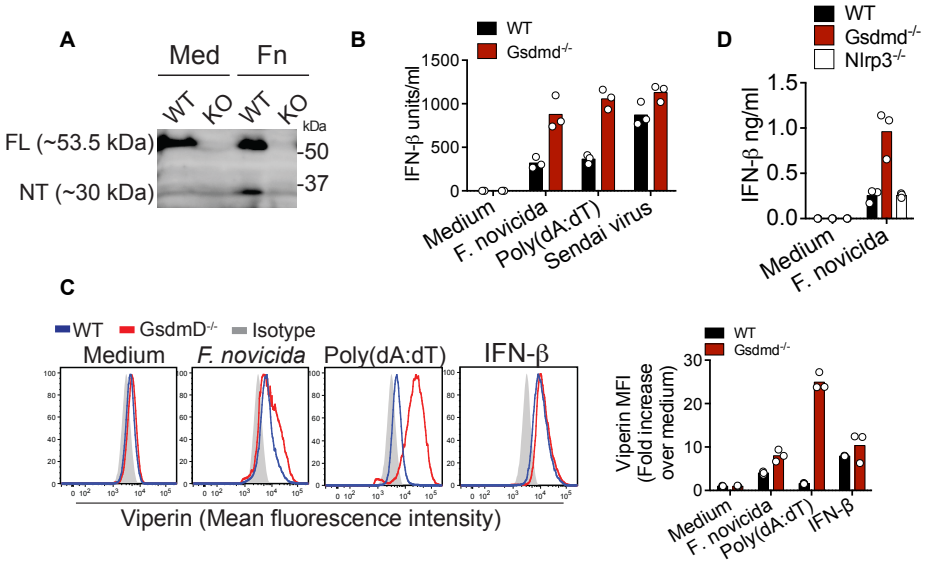

Fig. S1. Gasdermin D deficiency enhances cGAS-induced IFN-β response in primary BMDMs.
Related to Figure 2.

(A) Immunoblot showing full length (FL) and cleaved N terminal fragment (NT) of gasdermin D in the lysates of wild-type and Gsdmd$^{-/-}$ iBMDMs untreated (Med, medium) or infected with *F. novicida* (Fn) for 6 h.

(B) IFN-β levels in the supernatants of wild-type and Gsdmd$^{-/-}$ primary BMDMs stimulated with poly(dA:dT), *F. novicida* or Sendai virus. IFN-β levels are presented as units/ml or ng/ml depending upon the recombinant IFN-β standard used in the ELISA.

(C) Histograms displaying fluorescence intensities of viperin in WT and Gsdmd$^{-/-}$ iBMDMs stimulated with *F. novicida*, poly(dA:dT) or IFN-β. The fold increase in mean fluorescence intensity (MFI) of viperin in *F. novicida*-, poly(dA:dT)-, or IFN-β-treated over untreated cells (medium) is also shown.

(D) IFN-β levels in the supernatants of wild-type and Nlrp3$^{-/-}$ primary BMDMs stimulated with *F. novicida* for 6 h. Data presented as mean are from one experiment representative of three experiments. In the bar graphs, each dot represents a technical replicate.

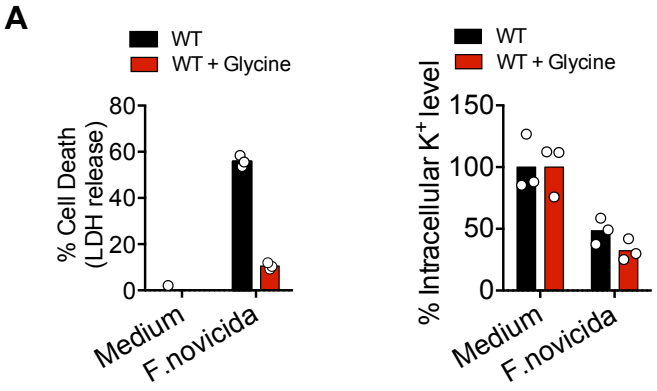

Figure S2.

Glycine treatment prevents pyroptotic lysis without altering K+ efflux.

(A) Cell Death (LDH release) and intracellular K^+ levels in uninfected (medium) or F. novicida-infected wild-type (WT) BMDMs in the presence or absence of 50mM glycine (assessed at 6h post-infection). Note that glycine treatment reduces LDH release without affecting K^+ efflux. Data presented as mean are from one experiment representative of three experiments. In the bar graphs, each dot represents a technical replicate.

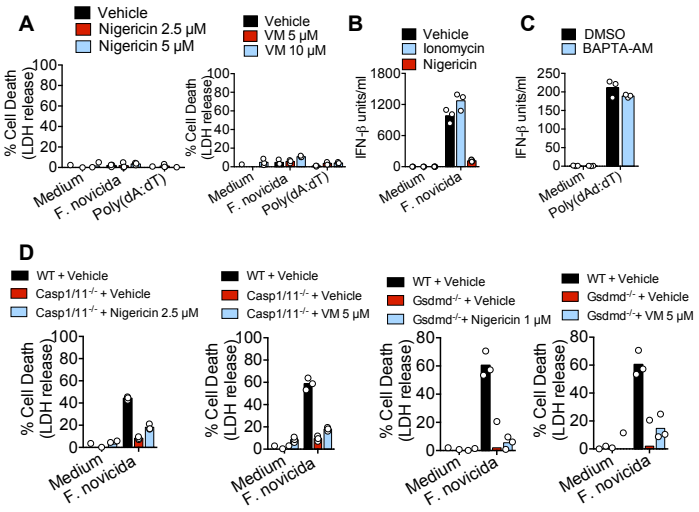

Figure S3.

Cytosolic DNA-induced IFN-b was not affected by calcium ionophore (ionomycin) and calcium chelator (BAPTA-AM). Related to Figure 5.

(A) LDH release (at 6h post-stimulation) by RAW macrophages stimulated with *F. novicida* (MOI of 50) or poly(dA:dT) and treated at 2h post-stimulations with vehicle (ethanol), 2.5 or 5 μM nigericin or 5 or 10 M valinomycin (VM) at indicated concentrations. (B) IFN-β secretion by RAW macrophages (measured at 6h post-infection) infected with *F. novicida* and treated with vehicle (ethanol), 1μM inomycin or 2.5 μM nigericin. (C) IFN-β secretion by BMDMs (measured at 6h post-infection transfected with poly(dA:dT), and treated with vehicle or 10μM BAPTA-AM. (D) LDH release by BMDMs of indicated genotypes (measured at 6h post-infection) infected with *F. novicida* and treated with vehicle (ethanol), nigericin or VM 2h post-infection at indicated concentrations. Data presented as mean are from one experiment representative of three experiments. In the bar graphs, each dot represents a technical replicate.

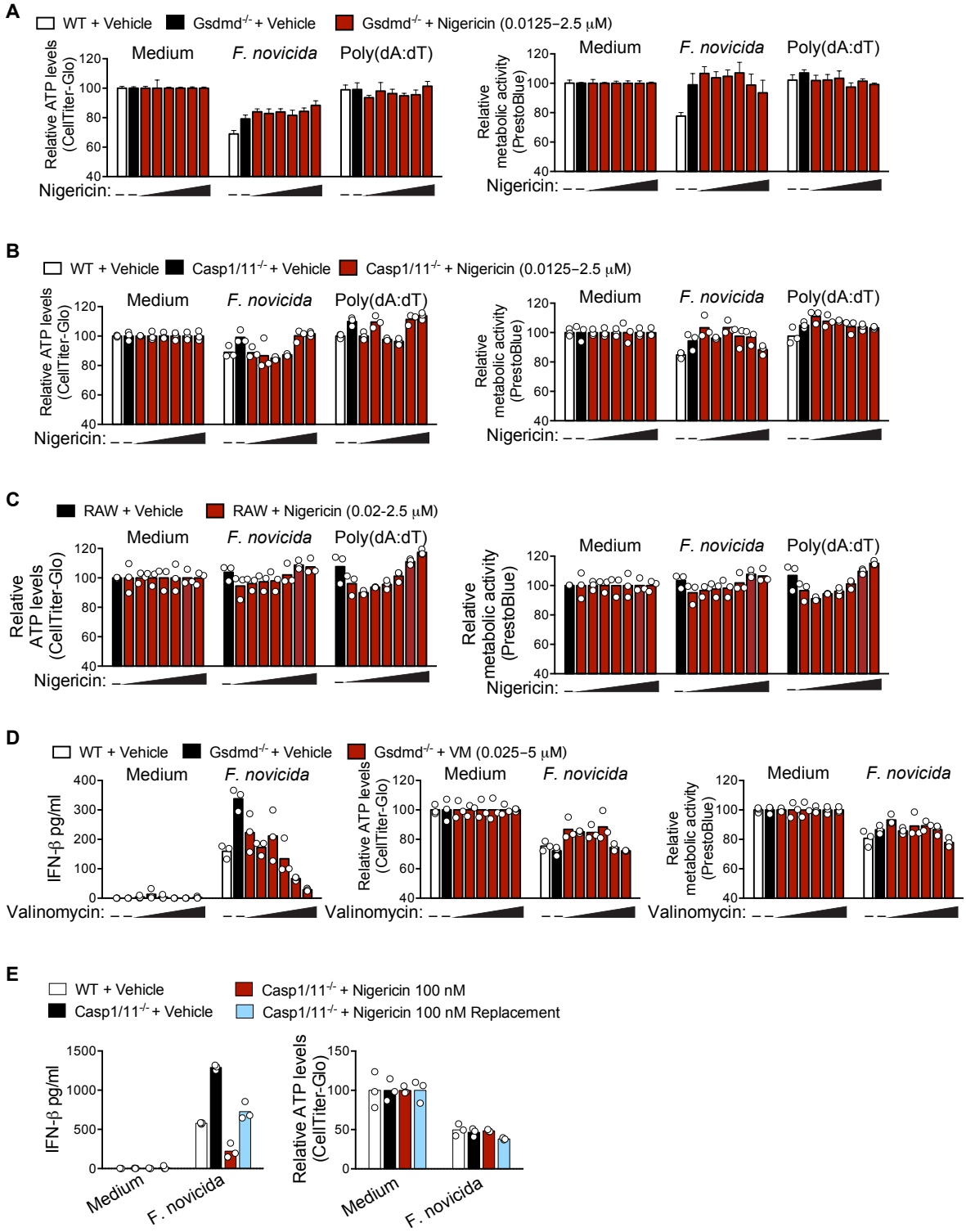
A
WT + Vehicle
Gsdmd-/- + Vehicle
Gsdmd-/- + Nigericin (0.0125–2.5 μM)
Relative ATP levels (CellTiter-Glo)
Relative metabolic activity (PrestoBlue)
Medium
F. novicida
Poly(dA:dT)
Nigericin:
B
WT + Vehicle
Casp1/11-/- + Vehicle
Casp1/11-/- + Nigericin (0.0125–2.5 μM)
C
RAW + Vehicle
RAW + Nigericin (0.02-2.5 μM)
D
WT + Vehicle
Gsdmd-/- + Vehicle
Gsdmd-/- + VM (0.025–5 μM)
IFN-β pg/ml
Valinomycin:
E
WT + Vehicle
Casp1/11-/- + Vehicle
Casp1/11-/- + Nigericin 100 nM
Casp1/11-/- + Nigericin 100 nM Replacement

Figure S4

Induction of K+ efflux in inflammasome-deficient macrophages is sufficient to restore cytosolic DNA induced type-I interferon response to wild-type levels. Related to Figure 5.

(A-C) Relative ATP levels and metabolic activity as measured by CellTiter-Glo and PrestoBlue assays, respectively, in indicated macrophages (at 6h post-stimulation) stimulated with *F. novicida* (MOI of 50) or poly(dA:dT) and treated at 1.5 - 2h post-stimulations with vehicle (ethanol), or increasing concentrations of nigericin (0.0125-2.5 μM). (D) IFN-β levels in supernatant of, intracellular ATP levela and metabolic activity as measured by CellTiter-Glo and PrestoBlue assays, respectively, in indicated macrophages (at 6h post-stimulation) stimulated with *F. novicida* (MOI of 50) or poly(dA:dT) and treated at 1.5 - 2h post-stimulations with vehicle (ethanol), or increasing concentrations of valinomycin (0.0125-2.5 μM). (E) IFN-β levels in supernatant of, intracellular ATP levels in indicated Casp1/11$^{-/-}$ BMDMs (at 6h post-stimulation) stimulated with *F. novicida* (MOI of 50) or poly(dA:dT). At 1.5h p.i., cells were treated with vehicle or nigericin (100 nM) and at 1h the media was replaced with media without nigericin. Data presented as mean are from one experiment representative of three experiments and each dot represents a technical replicate.

Chapter VI

Appendix

Results of the presented work have been published in Banerjee *et al.*, 2018.

Appendix: Table of Experimental Materials

Experimental Models: Organisms/Strains		
Mouse: C57BL/6J	The Jackson Laboratory	000664
Mouse: B6N.129S2-Casp1tm1Flv/J	The Jackson Laboratory	016621
Mouse: B6.129S7-I l1r1tm1Imx/J	The Jackson Laboratory	003245
Mouse: B6.129P2-I l18r1tm1Aki/J	The Jackson Laboratory	004131
Mouse: B6 GSDMD$^{-/-}$	Kayagaki *et al*., 2015. Genentech, CA	N/A
Mouse: B6 AIM2$^{-/-}$	Jones *et al*., 2010. Genentech, CA	N/A
Mouse: B6.129P2-AIM2Gt(CSG445)Byg/J	Rathinam *et al*., 2010. The Jackson Laboratory	013144
Mouse: B6 Caspase11$^{-/-}$	Kayagaki *et al*., 2011 Genentech, CA	N/A
Mouse: B6 Nlrp3$^{-/-}$	Rathinam *et al*., 2012.	N/A
Mouse: B6 Asc$^{-/-}$	Rathinam *et al*., 2010.	N/A
Mouse: B6 cGAS$^{-/-}$	Suschuk *et al*., 2016.	N/A
Oligonucleotides		
Primers for *F. novicida* mglA gene Forward: AGCGATATAGTCCGCATGATCC Reverse: TGGAAACATCGGAGGAAAGGG	This study N/A	
Sequence of DNA used in cGAS assay: ACA TCT AGT ACA TGT CTA GTC AGT ATC TAG	Dr. S.N. Sarkar	N/A

TGA TTA TCT AGA CAT ACA TCT AGT ACA TGT CTA GTC AGT ATC TAG TGA TTA TCT AGA CAT GGA CTC ATC C		
Recombinant DNA		
pMSCV-puro	Clontech	Cat# K1062-1
pMSCV-puro 2xFLAG-HA-GSDMD	This study (Genewiz)	N/A
pMSCV-puro 2xFLAG-HA I105N-GSDMD	This study (Genewiz)	N/A

REFERENCES

Ablasser A., Bauernfeind F., Hartmann G., Latz E., Fitzgerald K.A., Hornung V. (2009). RIG-I-dependent sensing of poly(dA:dT) through the induction of an RNA polymerase III-transcribed RNA intermediate. Nat. Immunol. 10:1065–1072.

Aglietti, R.A., Estevez, A., Gupta, A., Ramirez, M.G., Liu, P.S., Kayagaki, N., Ciferri, C., Dixit, V.M., and Dueber, E.C. (2016). GSDMD p30 elicited by caspase-11 during pyroptosis forms pores in membranes. Proceedings of the National Academy of Sciences 113, 7858–7863.

AhmadNejad P., Hacker H., Rutz M., Bauer S., Vabulas R.M., Wagner H. (2002).Bacteri al CpG-DNA and lipopolysaccharides activate Toll-like receptors at distinct cellular compartments. Eur. J. Immunol 32:1958–1968.

Auerbuch, V., Brockstedt, D.G., Meyer-Morse, N., O'Riordan, M., and Portnoy, D.A. (2004). Mice lacking the type I interferon receptor are resistant to Listeria monocytogenes. J Exp Med 200, 527–533.

Banerjee, I., Behl, B., Mendonca, M., Shrivastava, G., Russo, A J., Menoret, A., Patel N V., Vella, A T., Vanaja S K V., Sarkar S N., Fitzgerald K A., Rathinam V A K. (2018). Gasdermin D restrains type I interferon responses to cytosolic DNA by disrupting ionic homeostasis. Immunity 49, 413-426.

Barker, J. H., Weiss, J., Apicella, M. A. & Nauseef, W. M. Basis for the failure of Francisella tularensis lipopolysaccharide to prime human polymorphonuclear leukocytes. *Infect. Immun.* 74, 3277–3284 (2006).

Baum, R. *et al.* Cutting edge: AIM2 and endosomal TLRs differentially regulate arthritis and autoantibody production in DNase II-deficient mice. *J. Immunol. Baltim. Md 1950* 194, 873–877 (2015).

Bergsbaken, T., Fink, S.L., and Cookson, B.T. (2009). Pyroptosis: host cell death and inflammation. Nat. Rev. Microbiol. 7, 99–109.

Bossaller, L., Chiang, P.-I., Schmidt-Lauber, C., Ganesan, S., Kaiser, W.J., Rathinam, V.A.K., Mocarski, E.S., Subramanian, D., Green, D.R., Silverman, N., *et al*. (2012). Cutting edge: FAS (CD95) mediates noncanonical IL-1β and IL-18 maturation via

caspase-8 in an RIP3- independent manner. The Journal of Immunology 189, 5508–5512.

Broz P, von Moltke J, Jones JW, Vance RE, Monack DM. Differential requirement for Caspase-1 autoproteolysis in pathogen-induced cell death and cytokine processing. Cell host & microbe. 2010;8:471–483.

Burdette, D.L., Monroe, K.M., Sotelo-Troha, K., Iwig, J.S., Eckert, B., Hyodo, M., Hayakawa, Y., and Vance, R.E. (2011). STING is a direct innate immune sensor of cyclic di-GMP. Nature 478, 515–518. Chen, Q., Sun, L., and Chen, Z.J. (2016). Regulation and function of the cGAS–STING pathway of cytosolic DNA sensing. Nature Immunology 17, 1142–1149.

Chao, K. L., Kulakova, L. & Herzberg, O. Gene polymorphism linked to increased asthma and IBD risk alters gasdermin-B structure, a sulfatide and phosphoinositide binding protein. *Proc. Natl. Acad. Sci. U. S. A.* **114,** E1128–E1137 (2017).

Chen, Q. *et al.* Carcinoma-astrocyte gap junctions promote brain metastasis by cGAMP transfer. *Nature* **533**, 493–498 (2016).

Chen, K. W. *et al.* Noncanonical inflammasome signaling elicits GSDMD–dependent neutrophil extracellular traps. *Sci. Immunol.* **3,** eaar6676 (2018).

Chiu Y.H., Macmillan J.B., Chen Z.J. 2009. RNA polymerase III detects cytosolic DNA and induces type I interferons through the RIG-I pathway. Cell 138:576–591.

Clemens, D. L., Lee, B.-Y. & Horwitz, M. A. Virulent and Avirulent Strains of Francisella tularensis Prevent Acidification and Maturation of Their Phagosomes and Escape into the Cytoplasm in Human Macrophages. *Infect. Immun.* **72,** 3204–3217 (2004).

Collazo, C. M., Sher, A., Meierovics, A. I. & Elkins, K. L. Myeloid differentiation factor-88 (MyD88) is essential for control of primary in vivo Francisella tularensis LVS infection, but not for control of intra-macrophage bacterial replication. *Microbes Infect.* **8,** 779–790 (2006).

Conos, S.A., Chen, K.W., De Nardo, D., Hara, H., Whitehead, L., Núñez, G., Masters, S.L., Murphy, J.M., Schroder, K., Vaux, D.L., *et al*. (2017). Active MLKL triggers the

NLRP3 inflammasome in a cell-intrinsic manner. Proceedings of the National Academy of Sciences 114, E961–E969.

Corrales, L. *et al.* Direct activation of STING in the tumor microenvironment leads to potent and systemic tumor regression and immunity. *Cell Rep.* **11**, 1018–1030 (2015).

Corrales, L., Woo, S.-R., Williams, J.B., McWhirter, S.M., Dubensky, T.W., and Gajewski, T.F. (2016). Antagonism of the STING Pathway via Activation of the AIM2 Inflammasome by Intracellular DNA. The Journal of Immunology 196, 3191–3198.

Crow, M.K. (2016). Autoimmunity: Interferon α or β: which is the culprit in autoimmune disease? Nat Rev Rheumatol 12, 439–440. Crow, Y.J., and Manel, N. (2015). Aicardi-Goutieres syndrome and the type I interferonopathies. Nature Reviews Immunology 15, 429–440.

Cui, Y., Yu, H., Zheng, X., Peng, R., Wang, Q., Zhou, Y., Wang, R., Wang, J., Qu, B., Shen, N., *et al*. (2017). SENP7 Potentiates cGAS Activation by Relieving SUMO-Mediated Inhibition of Cytosolic DNA Sensing. PLoS Pathog 13, e1006156.

Demaria, O. *et al.* STING activation of tumor endothelial cells initiates spontaneous and therapeutic antitumor immunity. *Proc. Natl. Acad. Sci. USA* **112**, 15408–15413 (2015).

Delmaghani, S. *et al.* Mutations in the gene encoding pejvakin, a newly identified protein ofthe afferent auditory pathway, cause DFNB59 auditory neuropathy. *Nat. Genet.* **38,** 770–778 (2006).

Delmaghani, S. *et al.* Hypervulnerability to Sound Exposure through Impaired Adaptive Proliferation of Peroxisomes. *Cell* **163,** 894–906 (2015).

Di Micco, A. *et al.* AIM2 inflammasome is activated by pharmacological disruption of nuclear envelope integrity. *Proc. Natl. Acad. Sci. U. S. A.* **113,** E4671–4680 (2016).

Ding, J., Wang, K., Liu, W., She, Y., Sun, Q., Shi, J., Sun, H., Wang, D.-C., and Shao, F. (2016). Pore-forming activity and structural autoinhibition of the gasdermin family. Nature.

Dobbs, N. *et al.* STING Activation by Translocation from the ER Is Associated with Infectionand Autoinflammatory Disease. *Cell Host Microbe* **18,** 157–168 (2015).

Du, M. and Chen, Z.J. (2018). DNA-induced liquid phase condensation of cGAS activates innate immune signaling. Science.

Eil, R., Vodnala, S.K., Clever, D., Klebanoff, C.A., Sukumar, M., Pan, J.H., Palmer, D.C., Gros, A., Yamamoto, T.N., Patel, S.J., *et al*. (2016). Ionic immune suppression within the tumour microenvironment limits T cell effector function. Nature 537, 539–543.

Evavold, C.L., Ruan, J., Tan, Y., Xia, S., Wu, H., and Kagan, J.C. (2018). The Pore-Forming Protein GSDMD Regulates Interleukin-1 Secretion from Living Macrophages. Immunity

Fernandes-Alnemri T, *et al*. The pyroptosome: a supramolecular assembly of ASC dimers mediating inflammatory cell death via caspase-1 activation. Cell death and differentiation. 2007;14:1590–1604.

Fernandes-Alnemri, T., Yu, J.-W., Datta, P., Wu, J., and Alnemri, E.S. (2009). AIM2 activates the inflammasome and cell death in response to cytoplasmic DNA. Nature 458, 509–513.

Fernandes-Alnemri, T., Yu, J.-W., Juliana, C., Solorzano, L., Kang, S., Wu, J., Datta, P., McCormick, M., Huang, L., McDermott, E., *et al*. (2010). The AIM2 inflammasome is critical for innate immunity to Francisella tularensis. Nature Immunology 11, 385–393.

Fink, S.L., and Cookson, B.T. (2005). Apoptosis, pyroptosis, and necrosis: mechanistic description of dead and dying eukaryotic cells. Infect. Immun. 73, 1907–1916.

Fink, S. L. & Cookson, B. T. Caspase-1-dependent pore formation during pyroptosis leads to osmotic lysis of infected host macrophages. *Cell. Microbiol.* **8,** 1812–1825 (2006).

Fink, S.L., Bergsbaken, T., and Cookson, B.T. (2008). Anthrax lethal toxin and Salmonella elicit the common cell death pathway of caspase-1-dependent pyroptosis via distinct mechanisms. Proceedings of the National Academy of Sciences 105, 4312–4317.

Gohara, D.W., and Di Cera, E. (2016). Molecular Mechanisms of Enzyme Activation by Monovalent Cations. J Biol Chem 291, 20840–20848.

Gong, Y.-N., Guy, C., Olauson, H., Becker, J.U., Yang, M., Fitzgerald, P., Linkermann, A., and Green, D.R. (2017). ESCRT-III Acts Downstream of MLKL to Regulate Necroptotic Cell Death and Its Consequences. Cell 169, 286–300.e16.

Gray, E.E., Winship, D., Snyder, J.M., Child, S.J., Geballe, A.P., and Stetson, D.B. (2016). The AIM2-like Receptors Are Dispensable for the Interferon Response to Intracellular DNA. Immunity 45, 255–266.

Guo, H., König, R., Deng, M., Riess, M., Mo, J., Zhang, L., Petrucelli, A., Yoh, S.M., Barefoot, B., Samo, M., *et al*. (2016). NLRX1 Sequesters STING to Negatively Regulate the Interferon Response, Thereby Facilitating the Replication of HIV-1 and DNA Viruses. Cell Host & Microbe 19, 515–528.

Gutierrez, K.D., Davis, M.A., Daniels, B.P., Olsen, T.M., Ralli-Jain, P., Tait, S.W.G., Gale, M., and Oberst, A. (2017). MLKL Activation Triggers NLRP3-Mediated Processing and Release of IL-1β Independently of Gasdermin-D. J Immunol 198, 2156–2164.

Halapi, E. *et al.* A sequence variant on 17q21 is associated with age at onset and severity of asthma. *Eur. J. Hum. Genet. EJHG* **18,** 902–908 (2010).

Hall, J. D., Craven, R. R., Fuller, J. R., Pickles, R. J. & Kawula, T. H. Francisella tularensis replicates within alveolar type II epithelial cells in vitro and in vivo following inhalation. *Infect. Immun.* **75,** 1034–1039 (2007).

Hall, J. C. & Rosen, A. (2010).Type I interferons: crucial participants in disease amplification in autoimmunity. *Nat. Rev. Rheumatol.* 6, 40–49.

He, W.-T., Wan, H., Hu, L., Chen, P., Wang, X., Huang, Z., Yang, Z.-H., Zhong, C.-Q., and Han, J. (2015). GSDMD is an executor of pyroptosis and required for interleukin-1β secretion. Cell Res. 25, 1285–1298.

Henry, T., Kirimanjeswara, G.S., Ruby, T., Jones, J.W., Peng, K., Perret, M., Ho, L., Sauer, J.- D., Iwakura, Y., Metzger, D.W., *et al*. (2010). Type I IFN signaling constrains IL-17A/F secretion by gammadelta T cells during bacterial infections. The Journal of Immunology 184, 3755–3767.

Hornung, V., and Latz, E. (2010). Intracellular DNA recognition. Nature Reviews Immunology 10, 123–130.

Hornung, V., Ablasser, A., Charrel-Dennis, M., Bauernfeind, F., Horvath, G., Caffrey, D.R., Latz, E., and Fitzgerald, K.A. (2009). AIM2 recognizes cytosolic dsDNA and forms a caspase-1- activating inflammasome with ASC. Nature 458, 514–518.

Huang MT, *et al*. Critical role of apoptotic speck protein containing a caspase recruitment domain (ASC) and NLRP3 in causing necrosis and ASC speck formation induced by *Porphyromonas gingivalis* in human cells. Journal of immunology. 2009;182:2395–2404.

Jakobs, C., Perner, S. & Hornung, V. AIM2 Drives Joint Inflammation in a Self-DNA Triggered Model of Chronic Polyarthritis. *PLOS ONE* **10,** e0131702 (2015).

Jones, J.W., Kayagaki, N., Broz, P., Henry, T., Newton, K., O'Rourke, K., Chan, S., Dong, J., Qu, Y., Roose-Girma, M., *et al*. (2010). Absent in melanoma 2 is required for innate immune recognition of Francisella tularensis. Proceedings of the National Academy of Sciences 107, 9771–9776.

Kailasan Vanaja, S., Rathinam, V.A.K., Atianand, M.K., Kalantari, P., Skehan, B., Fitzgerald, K.A., and Leong, J.M. (2014). Bacterial RNA:DNA hybrids are activators of the NLRP3 inflammasome. Proceedings of the National Academy of Sciences 111, 7765–7770.

Kanaar, R., Wyman, C. (2008). DNA repair by the MRN complex: break it to make it. Cell. 135(1),14-6.

Kalliolias, G, D. & Ivashkiv, L. B. (2010). Overview of the biology of type I interferons. *Arthritis Res. Ther.* 12, S1

Kang, M.-J. *et al.* GSDMB/ORMDL3 variants contribute to asthma susceptibility and eosinophil-mediated bronchial hyperresponsiveness. *Hum. Immunol.* 73, 954–959 (2012).

Katsnelson, M.A., Rucker, L.G., Russo, H.M., and Dubyak, G.R. (2015). K^+ Efflux Agonists Induce NLRP3 Inflammasome Activation Independently of $Ca2^+$ Signaling. J Immunol 194, 3937–3952.

Kayagaki, N., Stowe, I.B., Lee, B.L., O'Rourke, K., Anderson, K., Warming, S., Cuellar, T., Haley, B., Roose-Girma, M., Phung, Q.T., *et al*. (2015). Caspase-11 cleaves

GSDMD for non-canonical inflammasome signaling. Nature 526, 666–671.

Kayagaki, N., Warming, S., Lamkanfi, M., Vande Walle, L., Louie, S., Dong, J., Newton, K., Qu, Y., Liu, J., Heldens, S., *et al*. (2011). Non-canonical inflammasome activation targets caspase- 11. Nature 479, 117–121.

Kerur N., Veettil M.V., SharmaWalia N., Bottero V., Sadagopan S., Otageri P., Chandran B. (2011). IFI16 acts as a nuclear pathogen sensor to induce the inflammasome in response to Kaposi sarcoma-associated herpesvirus infection. Cell Host Microbe. 9:363–375.

Konno, H., Konno, K., and Barber, G.N. (2013). Cyclic dinucleotides trigger ULK1 (ATG1) phosphorylation of STING to prevent sustained innate immune signaling. Cell 155, 688–698.

Kontaki, E., and Boumpas, D.T. (2010). Innate immunity in systemic lupus erythematosus: Sensing endogenous nucleic acids. Journal of Autoimmunity 35, 206–211.

Kovacs, S.B., and Miao, E.A. (2017). Gasdermins: Effectors of Pyroptosis. Trends Cell Biol. 27, 673–684.

Kranzusch, P.J., Lee, A.S.-Y., Berger, J.M., and Doudna, J.A. (2013). Structure of Human cGAS Reveals a Conserved Family of Second-Messenger Enzymes in Innate Immunity. Cell Rep 3, 1362–1368.

Lamkanfi, M., Dixit, V.M. Mechanisms and functions of inflammasomes . Cell . 2014 ;157:1013–1022.

Latz E., Schoenemeyer A., Visintin A., Fitzgerald K.A., Monks B.G., Knetter C.F., Lien E., Nilsen N.J., Espevik T., Golenbock D.T. 2004. TLR9 signals after translocating from the ER to CpG DNA in the lysosome. Nat Immunol 5:190–198.

Lee H.K., Lund J.M., Ramanathan B., Mizushima N., Iwasaki A. (2007). Autophagy-dependent viral recognition by plasmacytoid dendritic cells. Science 315:1398–1401.

Lei, Y., Wen, H., Yu, Y., Taxman, D.J., Zhang, L., Widman, D.G., Swanson, K.V., Wen, K.-W., Damania, B., Moore, C.B., *et al*. (2012). The mitochondrial proteins NLRX1 and TUFM form a complex that regulates type I interferon and autophagy. Immunity 36, 933–946.

Liang, Q., Seo, G.J., Choi, Y.J., Kwak, M.-J., Ge, J., Rodgers, M.A., Shi, M., Leslie, B.J., Hopfner, K.-P., Ha, T., *et al*. (2014). Crosstalk between the cGAS DNA sensor and Beclin-1 autophagy protein shapes innate antimicrobial immune responses. Cell Host & Microbe 15, 228–238.

Liu, X., Zhang, Z., Ruan, J., Pan, Y., Magupalli, V.G., Wu, H., and Lieberman, J. (2016). Inflammasome-activated GSDMD causes pyroptosis by forming membrane pores. Nature 535, 153–158.

Malik, M. *et al.* Toll-like receptor 2 is required for control of pulmonary infection with Francisella tularensis. *Infect. Immun.* **74,** 3657–3662 (2006).

Man, S.M., Karki, R., Malireddi, R.K.S., Neale, G., Vogel, P., Yamamoto, M., Lamkanfi, M., and Kanneganti, T.-D. (2015a). The transcription factor IRF1 and guanylate-binding proteins target activation of the AIM2 inflammasome by Francisella infection. Nature Immunology 16, 467–475.

Man, S.M., Zhu, Q., Zhu, L., Liu, Z., Karki, R., Malik, A., Sharma, D., Li, L., Malireddi, R.K.S., Gurung, P., *et al*. (2015b). Critical Role for the DNA Sensor AIM2 in Stem Cell Proliferation and Cancer. Cell 162, 45–58.

Martinon, F., Burns, K., and Tschopp, J. (2002). The inflammasome: a molecular platform triggering activation of inflammatory caspases and processing of proIL-beta. Mol Cell 10, 417– 426.

Mayer-Barber, K.D., Andrade, B.B., Oland, S.D., Amaral, E.P., Barber, D.L., Gonzales, J., Derrick, S.C., Shi, R., Kumar, N.P., Wei, W., *et al*. (2014). Host-directed therapy of tuberculosis based on interleukin-1 and type I interferon crosstalk. Nature 511, 99–103.

McNab, F., McNab, F., Mayer-Barber, K., Mayer-Barber, K., Sher, A., Sher, A., Wack, A., Wack, A., and O'Garra, A. (2015). Type I interferons in infectious disease. Nature Reviews Immunology 15, 87–103.

Meunier, E., Wallet, P., Dreier, R.F., Costanzo, S., Anton, L., Rühl, S., Dussurgey, S.,

Dick, M.S., Kistner, A., Rigard, M., *et al*. (2015). Guanylate-binding proteins promote activation of the AIM2 inflammasome during infection with Francisella novicida. Nature Immunology 16, 476– 484.

Moffat, T. The 'Childhood Obesity Epidemic': *Med. Anthropol. Q.* **24,** 1–21 (2010).

Moltke, von, J., Trinidad, N.J., Moayeri, M., Kintzer, A.F., Wang, S.B., van Rooijen, N., Brown, C.R., Krantz, B.A., Leppla, S.H., Gronert, K., *et al*. (2012). Rapid induction of inflammatory lipid mediators by the inflammasome in vivo. Nature 490, 107–111.

Muñoz-Planillo, R., Kuffa, P., Martínez-Colón, G., Smith, B.L., Rajendiran, T.M., and Núñez, G. (2013). K^+ Efflux Is the Common Trigger of NLRP3 Inflammasome Activation by Bacterial Toxins and Particulate Matter. Immunity 38, 1142–1153.

Nacionales, D. C. *et al.* (2007). Deficiency of the type I interferon receptor protects mice from experimental lupus. *Arthritis Rheum.* 56, 3770–3783.

Page, M.J., and Di Cera, E. (2006). Role of Na^+ and K^+ in Enzyme Function. Physiological Reviews 86, 1049–1092. Prindle, A., Liu, J., Asally, M., Ly, S., Garcia-Ojalvo, J., and Süel, G.M. (2015). Ion channels enable electrical communication in bacterial communities. Nature 527, 59–63.

Panganiban, R. A. *et al.* A functional splice variant associated with decreased asthma risk abolishes the ability of gasdermin B to induce epithelial cell pyroptosis. *J. Allergy Clin. Immunol.* (2018). doi:10.1016/j.jaci.2017.11.040

Platanias, L. C. (2005). Mechanisms of type-I- and type-II-interferon-mediated signalling. *Nat. Rev. Immunol.* 5, 375–386.

Raetz, C. R. H. *et al.* Discovery of new biosynthetic pathways: the lipid A story. *J. Lipid Res.* 50 Suppl, S103–108 (2009).

Rathinam, V.A.K., and Fitzgerald, K.A. (2016). Inflammasome Complexes: Emerging Mechanisms and Effector Functions. Cell 165, 792–800.

Rathinam, V.A.K., Jiang, Z., Waggoner, S.N., Sharma, S., Cole, L.E., Waggoner, L., Vanaja, S.K., Monks, B.G., Ganesan, S., Latz, E., *et al*. (2010). The AIM2 inflammasome is essential for host defense against cytosolic bacteria and DNA viruses.

Nature Immunology 11, 395–402.

Rathinam, V.A.K., Vanaja, S.K., Waggoner, L., Sokolovska, A., Becker, C., Stuart, L.M., Leong, J.M., and Fitzgerald, K.A. (2012). TRIF Licenses Caspase-11-Dependent NLRP3 Inflammasome Activation by Gram-Negative Bacteria. Cell 150, 606–619.

Rogers, C. *et al.* Cleavage of DFNA5 by caspase-3 during apoptosis mediates progression to secondary necrotic/pyroptotic cell death. *Nat. Commun.* **8,** 14128 (2017).

Roberts, Z.J., Goutagny, N., Perera, P.-Y., Kato, H., Kumar, H., Kawai, T., Akira, S., Savan, R., van Echo, D., Fitzgerald, K.A., *et al*. (2007). The chemotherapeutic agent DMXAA potently and specifically activates the TBK1-IRF-3 signaling axis. J Exp Med 204, 1559–1569.

Roth S., Rottach A., LotzHavla A.S., Laux V., Muschaweckh A., Gersting S.W., Muntau A.C., Hopfner K.P., Jin L., Vanness K., Petrini J.H., Drexler I., Leonhardt H., Ruland J. (2014). Rad50-CARD9 interactions link cytosolic DNA sensing to IL-1beta production. Nat. Immunol. 15:538–545.

Runkel, F. *et al.*, The dominant alopecia phenotypes Bareskin, Rex-denuded, and Reduced Coat 2 are caused by mutations in gasdermin 3. Genomics 84, 824-835 (2004).

Russo, H.M., Rathkey, J., Boyd-Tressler, A., Katsnelson, M.A., Abbott, D.W., and Dubyak, G.R.(2016). Active Caspase-1 Induces Plasma Membrane Pores That Precede Pyroptotic Lysis and Are Blocked by Lanthanides. The Journal of Immunology 197, 1353–1367.

Rühl, S., and Broz, P. (2015). Caspase-11 activates a canonical NLRP3 inflammasome by promoting K($^{+}$) efflux. European Journal of Immunology 45, 2927–2936.

Santic, M., Molmeret, M., Klose, K. E., Jones, S. & Kwaik, Y. A. The Francisella tularensis pathogenicity island protein IglC and its regulator MglA are essential for modulating phagosome biogenesis and subsequent bacterial escape into the cytoplasm. *Cell. Microbiol.* **7,** 969–979 (2005).

Sborgi, L., Rühl, S., Mulvihill, E., Pipercevic, J., Heilig, R., Stahlberg, H., Farady, C.J., Müller, D.J., Broz, P., and Hiller, S. (2016). GSDMD membrane pore formation constitutes the mechanism of pyroptotic cell death. Embo J. e201694696.

Schmid-Burgk, J.L., Gaidt, M.M., Schmidt, T., Ebert, T.S., Bartok, E., and Hornung, V. (2015). Caspase-4 mediates non-canonical activation of the NLRP3 inflammasome in human myeloid cells. European Journal of Immunology 45, 2911–2917.

Schneider, W.M., Chevillotte, M.D., and Rice, C.M. (2014). Interferon-Stimulated Genes: A Complex Web of Host Defenses. Annu Rev Immunol 32, 513–545.

Seo, G.J., Yang, A., Tan, B., Kim, S., Liang, Q., Choi, Y., Yuan, W., Feng, P., Park, H.-S., and Jung, J.U. (2015). Akt Kinase-Mediated Checkpoint of cGAS DNA Sensing Pathway. Cell Rep 13, 440–449.

Shi, J., Zhao, Y., Wang, K., Shi, X., Wang, Y., Huang, H., Zhuang, Y., Cai, T., Wang, F., and Shao, F. (2015). Cleavage of GSDMD by inflammatory caspases determines pyroptotic cell death. Nature 526, 660–665.

Stark, G. R. & Darnell, J. E. The JAK-STAT Pathway at Twenty (2012). *Immunity* 36, 503–514.

Storek, K.M., Gertsvolf, N.A., Ohlson, M.B., and Monack, D.M. (2015). cGAS and Ifi204 Cooperate To Produce Type I IFNs in Response to Francisella Infection. The Journal of Immunology 194, 3236–3245.

Sun, L., Wu, J., Du, F., Chen, X., and Chen, Z.J. (2013). Cyclic GMP-AMP synthase is a cytosolic DNA sensor that activates the type I interferon pathway. Science 339, 786–791.

Suschak, J.J., Wang, S., Fitzgerald, K.A., and Lu, S. (2016). A cGAS-Independent STING/IRF7 Pathway Mediates the Immunogenicity of DNA Vaccines. J Immunol 196, 310–316.

Sollberger, G. *et al.* GSDMD plays a vital role in the generation of neutrophil extracellulartraps. *Sci. Immunol.* **3,** (2018).

Vanaja, S.K., Russo, A.J., Behl, B., Banerjee, I., Yankova, M., Deshmukh, S.D., and

Rathinam, V.A.K. (2016). Bacterial Outer Membrane Vesicles Mediate Cytosolic Localization of LPS and Caspase-11 Activation. Cell 165, 1106–1119.

Wang, C., Guan, Y., Lv, M., Zhang, R., Guo, Z., Wei, X., Du, X., Yang, J., Li, T., Wan, Y., *et al*. (2018). Manganese Increases the Sensitivity of the cGAS-STING Pathway for Double-Stranded DNA and Is Required for the Host Defense against DNA Viruses. Immunity.

Wang, Y., Ning, X., Gao, P., Wu, S., Sha, M., Lv, M., Zhou, X., Gao, J., Fang, R., Meng, G., *et al*. (2017). Inflammasome Activation Triggers Caspase-1-Mediated Cleavage of cGAS to Regulate Responses to DNA Virus Infection. Immunity 46, 393–404.

Wassermann, R., Gulen, M.F., Sala, C., Perin, S.G., Lou, Y., Rybniker, J., Schmid-Burgk, J.L., Schmidt, T., Hornung, V., Cole, S.T., *et al*. (2015). Mycobacterium tuberculosis Differentially Activates cGAS- and Inflammasome-Dependent Intracellular Immune Responses through ESX- 1. Cell Host & Microbe 17, 799–810.

Wilson, J.E., Petrucelli, A.S., Chen, L., Koblansky, A.A., Truax, A.D., Oyama, Y., Rogers, A.B., Brickey, W.J., Wang, Y., Schneider, M., *et al*. (2015). Inflammasome-independent role of AIM2 in suppressing colon tumorigenesis via DNA-PK and Akt. Nat Med 21, 906–913.

Unterholzner L., Keating S.E., Baran M., Horan K.A., Jensen S.B., Sharma S., Sirois C., Jin T., Xiao T., Fitzgerald P., Paludan S., Bowie A.G. 2010. IFI16 is an innate immune sensor for intracellular DNA. Nat. Immunol. 11:997–1004.

Wu, J., Sun, L., Chen, X., Du, F., Shi, H., Chen, C., and Chen, Z.J. (2013). Cyclic GMP-AMP is an endogenous second messenger in innate immune signaling by cytosolic DNA. Science 339, 826–830.

Xia, P., Ye, B., Wang, S., Zhu, X., Du, Y., Xiong, Z., Tian, Y., and Fan, Z. (2016). Glutamylation of the DNA sensor cGAS regulates its binding and synthase activity in antiviral immunity. Nature Immunology 17, 369–378.

Yasuda K.,Richez C., Uccellini M.B., Richards R.J., Bonegio R.G., Akira S., Monestier M., Corley R.B., Viglianti G.A., Marshak-Rothstein A., Rifkin I.R. (2009). Requirement for DNA CpG content in TLR9-dependent dendritic cell activation induced by DNA-containing immune complexes. J Immunol 183:3109–3117.

Zhang, L., Mo, J., Swanson, K.V., Wen, H., Petrucelli, A., Gregory, S.M., Zhang, Z., Schneider, M., Jiang, Y., Fitzgerald, K.A., *et al*. (2014). NLRC3, a member of the NLR family of proteins, is a negative regulator of innate immune signaling induced by the DNA sensor STING. Immunity 40, 329–341.

Zhu, Q., Man, S.M., Karki, R., Malireddi, R.K.S., and Kanneganti, T.-D. (2018). Detrimental Type I Interferon Signaling Dominates Protective AIM2 Inflammasome Responses during Francisella novicida Infection. Cell Rep 22, 3168–3174.